

## **Distribution Agreement**

In presenting this thesis or dissertation as a partial fulfillment of the requirements for an advanced degree from Emory University, I hereby grant to Emory University and its agents the non-exclusive license to archive, make accessible, and display my thesis or dissertation in whole or in part in all forms of media, now or hereafter known, including display on the world wide web. I understand that I may select some access restrictions as part of the online submission of this thesis or dissertation. I retain all ownership rights to the copyright of the thesis or dissertation. I also retain the right to use in future works (such as articles or books) all or part of this thesis or dissertation.

Chiara Brust

4/20/2023

Spatial and Temporal Trends in PM<sub>2.5</sub> Concentrations in Guatemala Between 1998-2021

By

Chiara Brust

Degree to be awarded: MPH

Global Environmental Health

Eri Saikawa, PhD

Committee Chair

Spatial and Temporal Trends in PM<sub>2.5</sub> Concentrations in Guatemala Between 1998-2021

By

Chiara Brust

B.S. Biological Sciences  
Georgia State University  
2021

Thesis Committee Chair: Eri Saikawa, PhD

An abstract of  
a thesis submitted to the Faculty of the  
Rollins School of Public Health of Emory University  
in partial fulfillment of the requirements for the degree of  
Master of Public Health  
in Global Environmental Health  
2023

## Abstract

### Spatial and Temporal Trends in PM<sub>2.5</sub> Concentrations in Guatemala Between 1998-2021 By Chiara Brust

Analyzing air pollution trends in low-resourced countries may lead to discoveries of possible sources of contamination that can be reduced. However, there is insufficient data on ambient air pollution in Guatemala. To address this gap, satellite-derived data was analyzed for seasonal and spatial trends of ambient fine particulate matter (PM<sub>2.5</sub>) concentrations between 1998-2021, along with 2019 emissions sources that contributed to PM<sub>2.5</sub> mass. An on-the-ground monitor (e-sampler) in Jalapa, Guatemala also measured ambient PM<sub>2.5</sub> concentrations and other meteorological information such as wind speed and direction between 2018-2022. The satellite-derived results revealed that the annual average PM<sub>2.5</sub> concentrations for each department ranged between 16-44  $\mu\text{g}/\text{m}^3$ , which is 3-9x higher than the World Health Organization's annual mean target concentration of 5  $\mu\text{g}/\text{m}^3$ . The satellite data consistently indicated a spike in PM<sub>2.5</sub> concentrations in April, which was 1.5 times higher than the average for all months and was localized to areas with high biomass burning PM<sub>2.5</sub> contributions. These trends are also consistent with the e-sampler data, which also revealed spikes every April that were linked with winds coming from the northeast where there were high relative contributions to PM<sub>2.5</sub> from biomass burning. However, a paired t-test indicated that the satellite-derived data were significantly higher than the e-sampler measurements by about 20  $\mu\text{g}/\text{m}^3$ . Despite these absolute differences, the seasonal trends remain similar. Therefore, the satellite-derived data is useful for detecting patterns, but the absolute measurements must be bias-corrected to determine true exposure levels and more ground-based monitors must be deployed for better monitoring in Guatemala.

Spatial and Temporal Trends in PM<sub>2.5</sub> Concentrations in Guatemala Between 1998-2021

By

Chiara Brust

B.S. Biological Sciences  
Georgia State University  
2021

Thesis Committee Chair: Eri Saikawa, PhD

A thesis submitted to the Faculty of the  
Rollins School of Public Health of Emory University  
in partial fulfillment of the requirements for the degree of  
Master of Public Health  
in Global Environmental Health  
2023

## **Acknowledgements**

I would like to first thank Dr. Eri Saikawa for providing me with the best opportunities in environmental health research that I could have asked for. You welcomed me into the lab without a second thought and gave me the chance to learn skills that I will keep for the rest of my life. I am so glad that I was able to explore all of these many different fascinating projects at once while also developing relationships with the rest of the team. The Saikawa Lab has grown so much while I have been here, and it will continue to grow and do even more great and world-changing work in the future. Thank you to the entire Saikawa Lab team for the friendly and technical support that you all gave me. I am very excited to see where everyone's paths lead.

I would also like to thank the ECOLECTIVOS team, including Dr. Lisa Thompson, Dr. John McCracken, and everyone else who has contributed to this impressive project. This thesis would not exist without you all, and I know your hard work will continue to make an enormous impact in Guatemala.

Thank you also to Dr. Sarath Guttikunda for sharing his work with me and helping me analyze trends in PM<sub>2.5</sub> concentrations. You made a significant impact on this project that supported me tremendously.

Finally, I would like to thank everyone in my family for bearing with me as I completed this project. Your support throughout all of these years has led me to where I am today, and I will be forever grateful. My happiness is a direct result of all the love I feel from you.

# Table of Contents

<b>Introduction</b> .....	1
<b>Methods</b> .....	5
<b>E-Sampler</b> .....	5
<b>Satellite-Based PM &amp; Emissions Source Estimates</b> .....	7
<b>Satellite vs E-Sampler</b> .....	9
<b>Results</b> .....	10
<b>E-Sampler</b> .....	10
<b>Satellite-Derived PM &amp; Emissions Source Estimates</b> .....	15
<b>E-Sampler vs Satellite</b> .....	30
<b>Discussion</b> .....	31
<b>Conclusion</b> .....	34
<b>References:</b> .....	36

## Introduction

Guatemala, a country known for its breathtaking landscapes and rich cultural heritage, is facing an invisible foe that is silently affecting the health of its citizens. Air pollution, primarily caused by anthropogenic activities, is a pervasive problem that poses a serious risk to public health. Particulate matter with an aerodynamic diameter of less than  $2.5\mu\text{m}$  ( $\text{PM}_{2.5}$ ) is a particularly dangerous type of air pollutant that can penetrate deep into the lungs, causing adverse health effects (Valavanidis et al., 2008). Despite the gravity of the situation, there is a lack of comprehensive data on ambient air pollution in Guatemala, which makes it difficult to identify sources of pollution that can be mitigated. However, the potential impact of such research cannot be overstated, as exposure to ambient particulate matter is responsible for an estimated 4.5 million deaths worldwide each year (Fuller et al., 2022). This makes it the 7th leading risk of attributable disability adjusted life years (GBD Risk Factor Collaborators, 2020). In this context, analyzing seasonal and spatial ambient particulate matter (PM) trends in Guatemala can provide critical insights that could lead to effective interventions to improve air quality and safeguard public health.

The short-term effects of elevated exposure to air pollution may be as mild as irritation of the respiratory passages or as severe as pneumonia and heart difficulties, while long-term exposure may cause cancer or harm on the nervous and reproductive systems (Manisalidis et al., 2020). The sources of air pollution primarily stem from industrialized practices such as metallurgy, oil refinement, and automobiles along with natural sources such as volcanoes, although the latter contributes a small relative proportion (Manisalidis et al., 2020). In addition to industrial and natural sources, biomass burning for agricultural practices such as crop burning in

field cultivation also contributes substantially (Bellarby et al., 2008). Biomass burning includes both natural and anthropogenic origins such as forest fires and agricultural waste burning. Within the umbrella of agricultural waste is crop residue, which is waste generated as a byproduct of harvesting crops. When crops are harvested and processed, non-edible components such as stalks, stems, and leaves are left out (Obi et al., 2016). Oftentimes, these harvest byproducts are burned; up to 32% of total greenhouse gas emissions from man-made sources are attributed to the agricultural industry, and 12% of these emissions are from biomass burning alone (Bellarby et al., 2008).

As food demand grows as a result of the increasing world population and rise of economies, there is an expanding need for high-throughput agricultural practices (FAO, 2014). However, this intensity is forcing farmers to practice unsustainable land management techniques. In some parts of Guatemala, farmers must use the same field from the previous cultivation cycle without incorporating a fallow period, or periods without cultivation, due to land shortages. This makes crop burning an attractive option in order to quickly clear fields and get rid of harvest waste before the next season's crop (Pérez Orozco, 2014). Despite practicing crop residue burning, many farmers understand the negative consequences of this method and note adverse health effects such as coughing, respiratory allergies, and headaches by their families when they burn crops. They also see a reduction in productivity due to illness and more roadway accidents from heavy smog (Raza et al., 2022). Regardless, the ease and low upfront costs of burning crop residue make it a common practice in many developing countries around the world. In Guatemala, agriculture is a predominant industry and stands as a major livelihood for Guatemalan households through the production of maize, coffee, sugarcane, and African palm (Lopez-Ridaura et al., 2019). However, a 2014 report found that 70% of farmers in an agrarian

Guatemalan community burn their crops, and, in 2020, at least 450 square kilometers of Guatemalan land were affected by fires (Pérez Orozco, 2014; *Guatemala Fires 2020* / *NASA Applied Sciences*, 2020). Due to the high levels of emissions from crop burning, this practice must be contributing to the estimated 4,000 deaths and \$1.4 billion in health damages per year in Guatemala alone from ambient PM<sub>2.5</sub> exposure (World Bank, 2020; Bellarby et al., 2008).

Despite the known health effects and the need to identify population exposure to air pollution, there are stark differences in ambient air quality monitoring between the Global North and the Global South. For example, North America has about one monitor for every 400,000 people. On the other hand, Sub-Saharan Africa has one monitor per 15.9 million people (Pinder et al., 2019). To our knowledge, only two previous studies have set up ground-based ambient PM<sub>2.5</sub> monitors in Guatemala, and both of these studies took place over 20 years ago back in 2000 and 2002 within a relatively short time frame (Naeher et al., 2000; Shendell & Naeher, 2002). The 2000 study by Naeher et al. (2000) was primarily focused on household air pollution related to cookstoves, but they also included street-level ambient monitoring that involved a research technician wearing a personal monitoring device as they walked through the city in between sampling homes. The average street-level PM<sub>2.5</sub> concentrations for all villages, all households, and all mealtimes combined for this study was 230 µg/m<sup>3</sup>. Similarly, the study conducted by Shendell & Naeher (2002) involved a technician transporting the monitoring device throughout city streets for about 4-6 hours at a time for a total of 39 days in three different cities near the capital of Guatemala. The integrated average for this study was a PM<sub>2.5</sub> concentration of approximately 41.56 µg/m<sup>3</sup>. Along with the two studies previously mentioned, there are eight ground-based sensors scattered throughout the country that are developed by PurpleAir and managed by community scientists ([www.purpleair.com](http://www.purpleair.com)).

This incomplete monitoring network leaves populations living in the Global South at a higher risk. Therefore, the purpose of this study is to contribute to the growing need for ambient  $PM_{2.5}$  monitoring in the Global South and identify potential sources of emissions in Guatemala. This study will also identify seasonal and spatial trends in  $PM_{2.5}$  concentrations between 1998-2021 in Guatemala, along with the magnitude of  $PM_{2.5}$  concentrations that people in this country are exposed to. To address these questions, we will pursue the following specific aims: (1) Conduct a spatial and temporal analysis of satellite-estimated air pollution concentrations; (2) Conduct a temporal analysis of on-the-ground monitor data; and (3) Analyze relative source emissions contributions. To accomplish these goals, there are over twenty years of ambient  $PM_{2.5}$  data that is publicly available for Guatemala from satellite-derived models (van Donkelaar et al., 2021). Therefore, this satellite data are used to identify seasonal and spatial trends in  $PM_{2.5}$  between 1998-2021. The authors from this same data source also had information on the relative contributions of source emissions such as biomass burning and transportation that can be used to determine what sources are creating high PM events (McDuffie et al., 2021). In addition, this study analyzes four years (2018- 2022) of ambient observational data in Jalapa, Guatemala where an on-the-ground monitor (e-sampler developed by Met One Instruments, Inc.) measured  $PM_{2.5}$  concentrations every 5 minutes along with additional variables, such as wind speed and direction. Combined with the meteorological data on site, we will have a better sense of where peaks in  $PM_{2.5}$  are stemming from and potentially estimate the source and origin of pollution events.

## Methods

We performed all subsequent analyses using R statistical software version 4.2.1 (R Core Team, 2022) and R Studio Desktop (RStudio Team, 2020).

### E-Sampler

#### Data Collection

The on-the-ground ambient air quality monitor (E-Sampler 9800, Met One Instruments, Inc.) was located on the roof (1000 m ASL) of a wellness center called CAP Sanyuyo in Jalapa, Guatemala (latitude: 14.6386, longitude: -90.1511), as shown in Figure 1. This e-sampler is a nephelometer that measures real-time PM<sub>2.5</sub> concentrations in the air using forward laser light scatter (<https://metone.com/products/e-sampler/>). During the period between August 2018 and August 2022, the e-sampler measured PM<sub>2.5</sub> concentrations along with other meteorological information such as wind speed and direction in Jalapa, Guatemala. Additional data collected include the real-time sample flow rate, ambient temperature, ambient barometric pressure, ambient relative humidity, internal filter sample relative humidity, and battery voltage. The e-sampler collected measurements every five minutes except for periods in between e-sampler maintenance (changing out the tape).

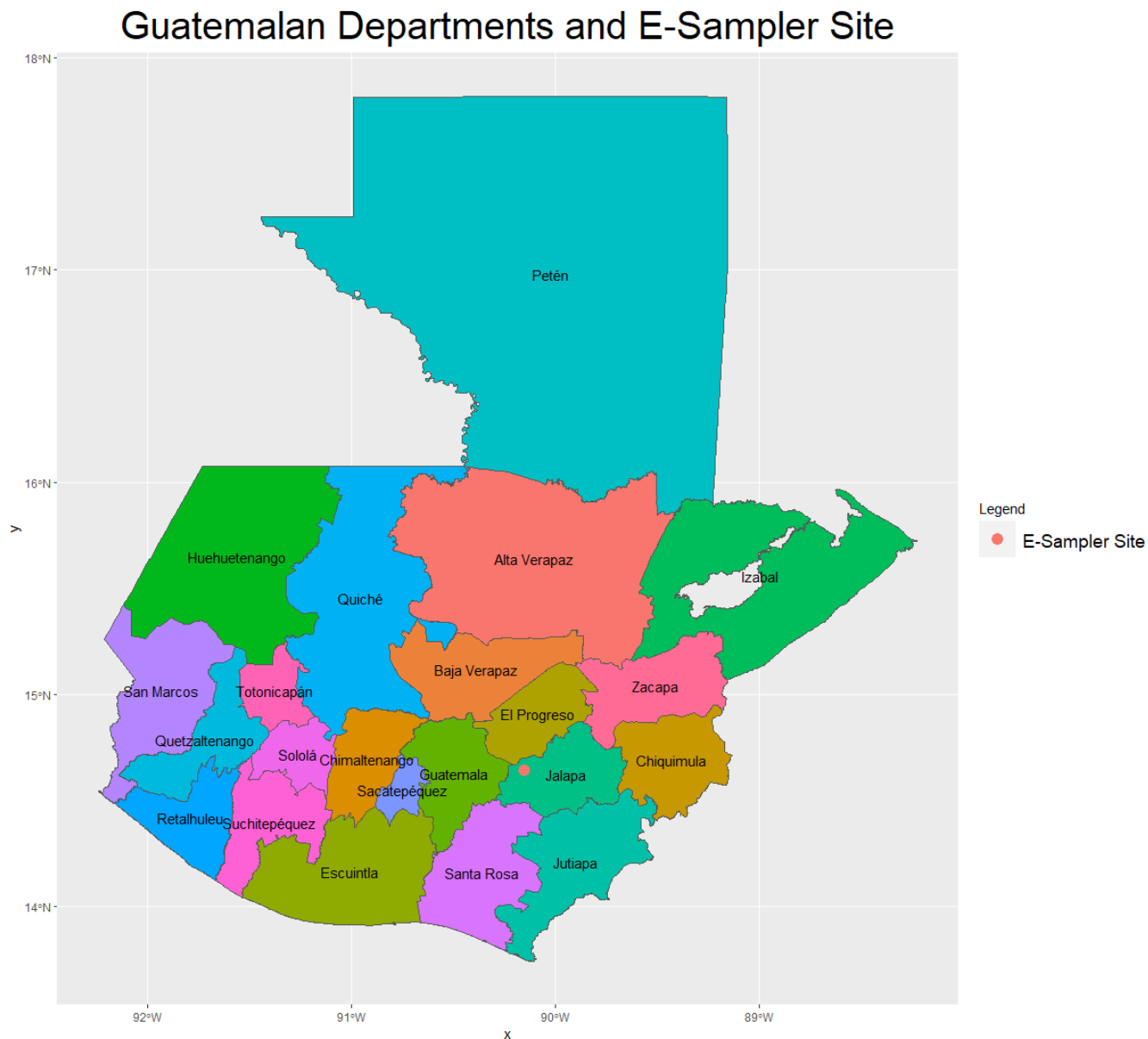


**Fig 1.** Map of each Guatemalan Department. The e-sampler site is indicated by a red point in Jalapa, Guatemala.

### Data Processing

Excluding a period between February 1, 2021, to November 25, 2021, when an equipment malfunction occurred, there were 9.05% of missing data attributable to reasons such as monthly maintenance and temporary pressure sensor failures. To adjust for missing observations within each hour, we utilized the openair R package version 2.11 (Carslaw &

Ropkins, 2012) to calculate the hourly averages only when a certain number of observations were present within the hour. For example, a data threshold of 100% signifies that every 5-minute observation within the hour must be present for the average to be calculated. Conversely, a data threshold of 0% signifies that the hourly average will be calculated regardless of the number of observations available within the specified time period. When using the strictest data threshold (100%) compared to not using one at all (0%), there was a statistically significant difference in monthly average  $PM_{2.5}$  concentrations ( $p\text{-value} = 5.652 \times 10^{-5}$ ) when performing a paired t-test. Despite this, the mean difference in  $PM_{2.5}$  concentrations between these two data thresholds was only  $0.022 \mu\text{g}/\text{m}^3$ , so we used 100% data threshold averages for all subsequent statistical tests and plots related to the e-sampler data.

Over the e-sampler study period of August 2018 to August 2022, we calculated basic descriptive statistics from the hourly and monthly average  $PM_{2.5}$  concentrations including the mean, maximum, standard deviations, and 25%, 50%, and 75% quartiles. We created a time series line plot to show trends in monthly-averaged  $PM_{2.5}$  concentrations over the years and also used the `timeVariation` function from the `openair` R package to plot diurnal, day of the week, and monthly variations. We used the `polarPlot` function from this package to illustrate the relationship between  $PM_{2.5}$  concentrations and wind speed and direction by creating a bivariate polar plot that uses generalized additive models. To visualize the seasonal variations of the e-sampler data, the `polarAnnulus` function from the `openair` package was used as well. This was done to clearly show  $PM_{2.5}$  concentration by wind direction as a function of time.

## **Satellite-Based PM & Emissions Source Estimates**

### **Data Collection**

For the rest of the country, we utilized the latest global/regional surface PM estimates developed by Washington University in St. Louis (version V5GL03) at a  $0.1^\circ \times 0.1^\circ$  resolution, which was created through the combination of aerosol optical depth retrievals from NASA MODIS, MISR, and SeaWiFS instruments and the GEOS-Chem chemical transport model before being calibrated using on-the-ground observations through a geographically-weighted regression (van Donkelaar et al., 2021). This available satellite-derived data contained monthly- and yearly-averaged estimates of  $PM_{2.5}$  concentrations from January 1998 to December 2021. Furthermore, we applied data from the Global Burden of Disease-Mapping of Air Pollution Sources (GBD-MAPS) study, which combined the global GEOS-Chem 3D chemical transport model with  $PM_{2.5}$  exposure estimates and epidemiological relationships to determine the relative contributions of emissions sources to ambient  $PM_{2.5}$  mass in 2019 (McDuffie et al., 2021). For our analysis, we utilized Guttikunda & Ka's (2022) annual-averaged aggregated version of the GBD-MAPS study, which was a combination of the 20 source categories from the original study into 10 broader categories, which amounted to the following: Anthropogenic dust, Wind erosion (dust storms), Waste burning, All commercial and residential cooking, lighting, and heating, All transport (excluding aviation), Energy generation, All industries and product use, Biomass burning (including forest fires and agricultural waste burning), Agricultural activities (excluding agricultural waste burning), and All others.

### **Data Processing**

For the satellite-based PM estimates, we calculated descriptive statistics and created monthly and yearly time series line plots of  $PM_{2.5}$  over the period from January 1998- December 2021 for all of Guatemala and each of its departments. As can be seen in figure 1, there are 22 departments that make up Guatemala. To eliminate any confusion, there is a department within

Guatemala called Guatemala, so any further mention of Guatemala will be related to the country itself and not the department unless otherwise specified. To reduce noise and assess overall monthly trends, we calculated the average of each month across all the years. From these monthly and yearly averages, we developed spatial plots illustrating the variability in monthly and yearly PM<sub>2.5</sub> using the R package ggplot2 version 3.4.0 (Wickham, 2016). To do this, we converted the gridded data into a raster and linearly interpolated it before superimposing it onto the Guatemala shapefile. In addition, we estimated yearly population-weighted PM<sub>2.5</sub> exposures by taking the sum of the product of the population and PM<sub>2.5</sub> concentrations at each grid and dividing it by the total population in the given department or country. We calculated descriptive statistics of these weighted exposures for the entire country (for each year) and for each department (combined average of all the years) and created a bar graph to illustrate the difference in population-weighted exposures for each department. From Guttikunda & Ka's (2022) aggregated version of the GBD-MAPS study data, we plotted the spatial distribution of the relative contributions from the 10 different PM<sub>2.5</sub> emissions source categories. We did this by plotting the relative contributions of each emissions source in the same manner as we did with the satellite-based PM estimates by converting the gridded data into a raster and linearly interpolating it before superimposing it onto the Guatemala shapefile.

### **Satellite vs E-Sampler**

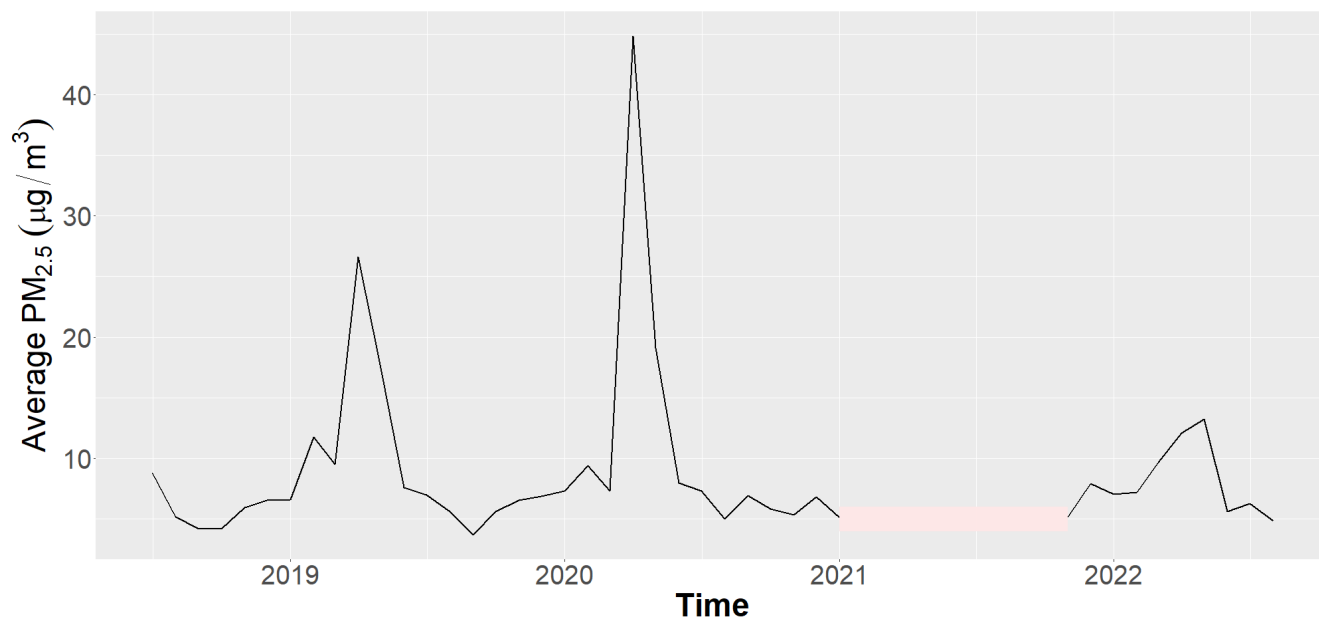
When comparing the satellite-derived data to the e-sampler measurements, we specifically used the coordinate at latitude 14.65 and longitude -90.15, which were the closest available to the e-sampler site in Jalapa. We performed a paired t-test to compare the available e-sampler data with the satellite-derived data between 2018-2021 using the satellite-derived data at both a fine (0.01° x 0.01°) and coarse (0.1° x 0.1°) resolution. In addition, we created a time

series line plot with the e-sampler data and the finer resolution satellite-derived data on the same figure to visualize the differences between the two data sources.

## **Results**

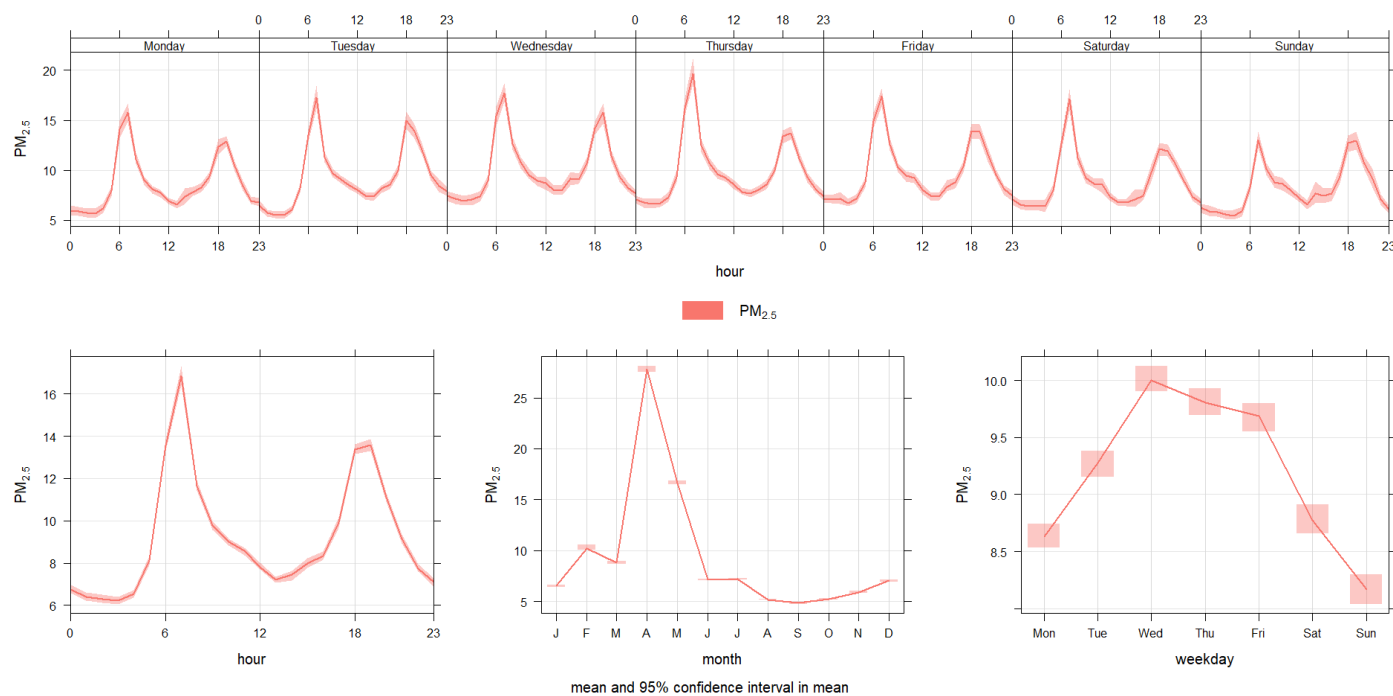
### **E-Sampler**

Figure 2 shows the monthly-averaged PM<sub>2.5</sub> concentrations between August 2018-August 2022. This plot reveals two major spikes in April of 2019 and 2020 that reach 27  $\mu\text{g}/\text{m}^3$  and 45  $\mu\text{g}/\text{m}^3$ , respectively. Aside from the spring months, the annual average PM<sub>2.5</sub> concentration is only about 6.5  $\mu\text{g}/\text{m}^3$ , which is four times lower than the spring 2019 spike and seven times lower than the spring 2020 spike. This shows how drastic the changes in PM<sub>2.5</sub> concentrations are during the spring. The maximum daily average was 102  $\mu\text{g}/\text{m}^3$  on April 26, 2020. Looking at the raw 5-minute data, the maximum value recorded by the e-sampler was 835  $\mu\text{g}/\text{m}^3$  on the afternoon of January 16, 2021.



**Fig 2.** Trends in monthly-averaged PM<sub>2.5</sub> concentrations in Guatemala over 1998-2021. The red bar represents the time period in 2021 when an e-sampler equipment malfunction resulted in lost data.

In Figure 3, we are able to see the diurnal, day of the week, and monthly variation in PM<sub>2.5</sub> concentrations. The diurnal variation seems to be very similar for each day of the week with two major peaks occurring in the morning and evening hours. Aside from Sunday when both peaks are of similar magnitude, the morning peak for each day of the week is higher than the evening peak. Throughout the week, the daily PM<sub>2.5</sub> concentrations are at their lowest near the weekends then peak on Wednesdays. The monthly time series plot shows that there is a trend of higher PM<sub>2.5</sub> concentrations in April across the entire study time period, and the average April concentration is about 28 µg/m<sup>3</sup>.



**Fig 3.** Change in PM<sub>2.5</sub> concentrations from the e-sampler data on a daily (top), hourly (bottom left), monthly (bottom middle), and weekly (bottom right) basis.

The polar annulus graph (Figure 4) clearly illustrates that there are peak PM<sub>2.5</sub> concentrations during the spring months. As seen through the blue and green color gradients, this figure shows relatively low concentrations through all months except for select months in the springtime that show distinct red color bands. We can see that there are colors representing higher concentrations on the bottom half of the figure, which indicates that higher concentrations are coming from southern sources. The red ring around the spring is, however, still apparent even when the wind is blowing from the north, which indicates that is also another emissions source that is located to the north of the site in the spring that is contributing to higher PM<sub>2.5</sub> concentrations during that time compared to the other months.

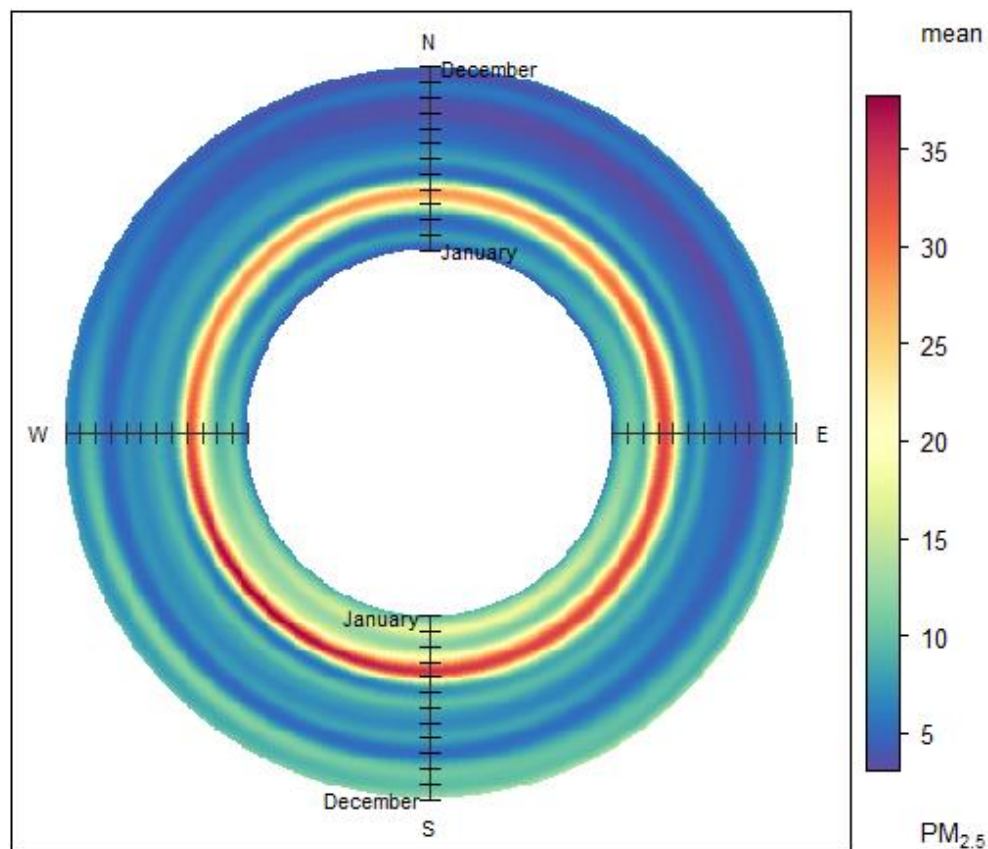


**Fig 4.** Polar Annulus plot of  $PM_{2.5}$  concentrations by wind direction and time between 2018-2022.

The polar plot (Figure 5) shows  $PM_{2.5}$  concentrations as a function of both wind speed and wind direction. Quadrants with higher  $PM_{2.5}$  concentrations (in red) indicate where the winds transporting  $PM_{2.5}$  are coming from, not where the winds are going towards. The positions of the representative colors on the concentric rings indicate the wind speed at which those concentrations are typically found. In the spring, we can see in Figure 5 that the higher  $PM_{2.5}$  concentrations tend to be coming from both southern and northern sources. The wind speeds are low when the higher  $PM_{2.5}$  concentrations are coming from southern sources, but the wind speeds are greater when the higher  $PM_{2.5}$  concentrations are coming from northern sources. This

could indicate that there is an emissions source located near the e-sampler to the south as well as another source that is located further away from the e-sampler and to the north. In autumn, most of the higher  $PM_{2.5}$  concentrations come from sources on only the south side of the e-sampler, and the wind speed is relatively low. During the winter and summer, the wind speeds are higher than the other two seasons, suggesting that the sources of higher  $PM_{2.5}$  concentrations during these months are from  $PM_{2.5}$  that has been transported over longer distances rather than being local to the area. These sources are on the south side of the site during these months and tend to originate from the southeast in the summer and southwest in the winter.

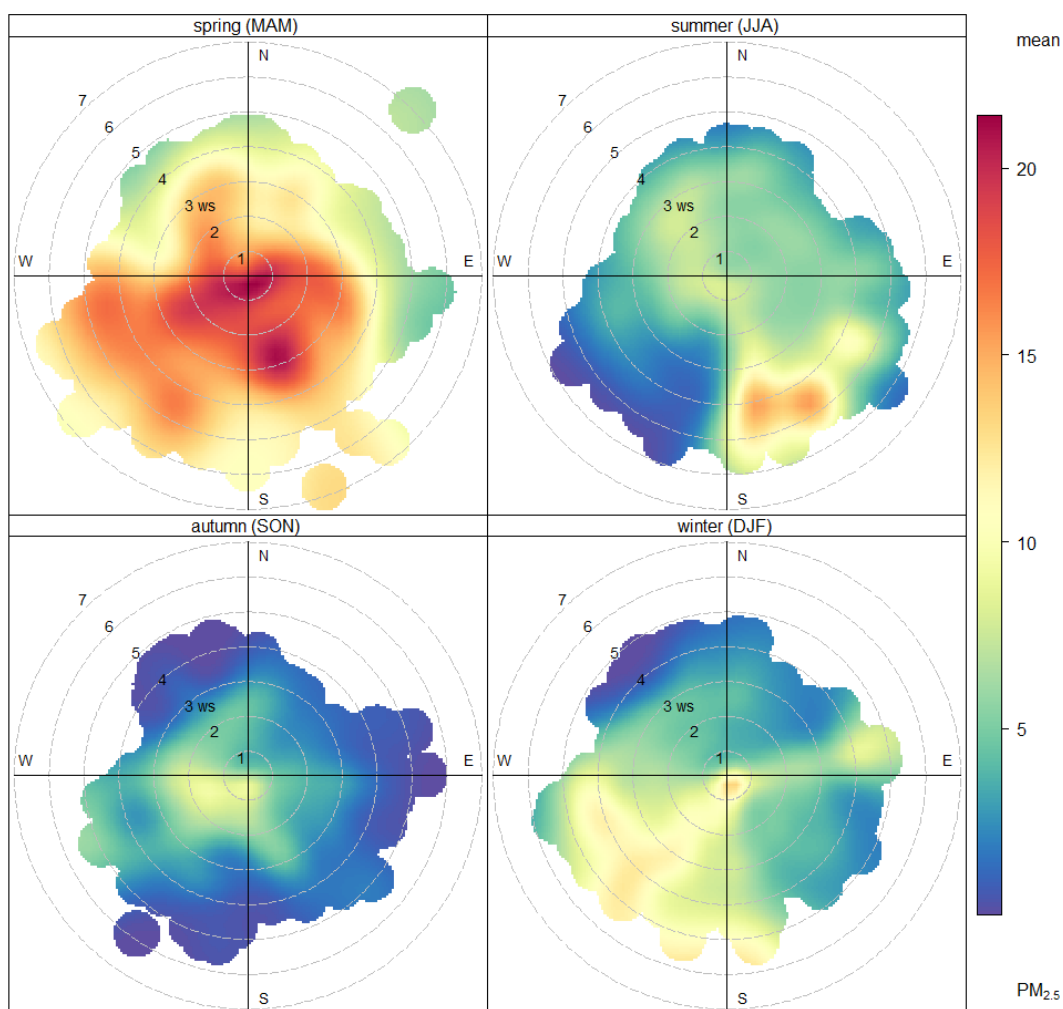


**Fig 5.** Polar plot of PM<sub>2.5</sub> concentrations by both wind speed and direction over 2018-2022, separated by season. Spring (top left), summer (top right), autumn (bottom left), and winter (bottom right) are shown.

### Satellite-Derived PM & Emissions Source Estimates

Similar to the e-sampler, the time series analysis (Figure 6 & Table 1) of the satellite-derived data across 1998- 2021 reveals the same monthly trend of concentration spikes occurring in April. The average PM<sub>2.5</sub> concentration in April from the satellite-derived data is 39  $\mu\text{g}/\text{m}^3$ . On the other hand, the month of August has the lowest concentrations at 20  $\mu\text{g}/\text{m}^3$ . It appears that September-December have very similar averages at around 22  $\mu\text{g}/\text{m}^3$ , while the overall average for all months is 26  $\mu\text{g}/\text{m}^3$ .

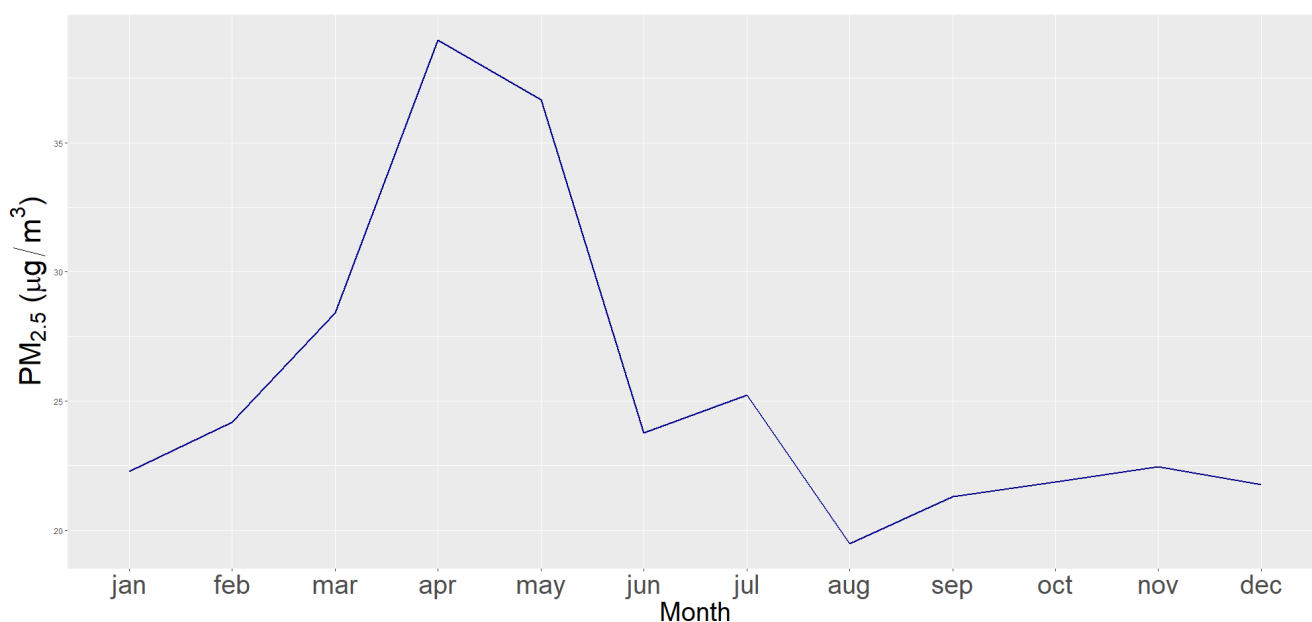


**Fig 6.** Trends in monthly-averaged PM<sub>2.5</sub> in Guatemala over 1998-2021.

**Table 1.** Summary statistics of the monthly average PM<sub>2.5</sub> concentrations between 1998-2021 for the entire country of Guatemala. The average, standard deviation (SD), minimum (Min), first quartile (Q1), median (Med), third quartile (Q3), and maximum (Max) are listed.

<b>Month</b>	<b>Average</b>	<b>SD</b>	<b>Min</b>	<b>Q1</b>	<b>Med</b>	<b>Q3</b>	<b>Max</b>
<b>Jan</b>	22.28	1.97	18.92	20.93	21.78	24.09	25.62
<b>Feb</b>	24.17	2.01	20.5	22.65	23.94	25.5	29.2
<b>Mar</b>	28.4	6.1	23.18	25.3	26.38	29.32	49.89
<b>Apr</b>	38.98	8.97	29.94	32.98	35.39	40.28	62.61
<b>May</b>	36.66	9.34	22.65	31.53	34.32	41.95	64.12
<b>Jun</b>	23.77	2.32	19.3	22.07	24.25	25.3	27.93
<b>Jul</b>	25.22	3.54	18.47	22.49	24.96	27.79	31.9
<b>Aug</b>	19.48	1.74	16.24	18.3	19.03	20.58	23.16
<b>Sep</b>	21.3	2.09	16.6	20.54	20.93	22.54	25.15
<b>Oct</b>	21.88	2.76	15.42	20.88	21.61	23.11	29.56
<b>Nov</b>	22.45	1.47	19.63	21.65	22.7	23.34	25.32
<b>Dec</b>	21.78	1.99	16.07	21.02	22.11	22.93	24.9

In Figure 7, we can see that the yearly averages in Guatemala vary, especially during the first few years of the available satellite-derived data when the PM<sub>2.5</sub> concentrations fluctuate between about 20  $\mu\text{g}/\text{m}^3$  and 30  $\mu\text{g}/\text{m}^3$ . This begins to level out after 2005 and remains relatively steady at around 25  $\mu\text{g}/\text{m}^3$ . The overall annual average concentration across all the years between 1998-2021 is 26  $\mu\text{g}/\text{m}^3$ .

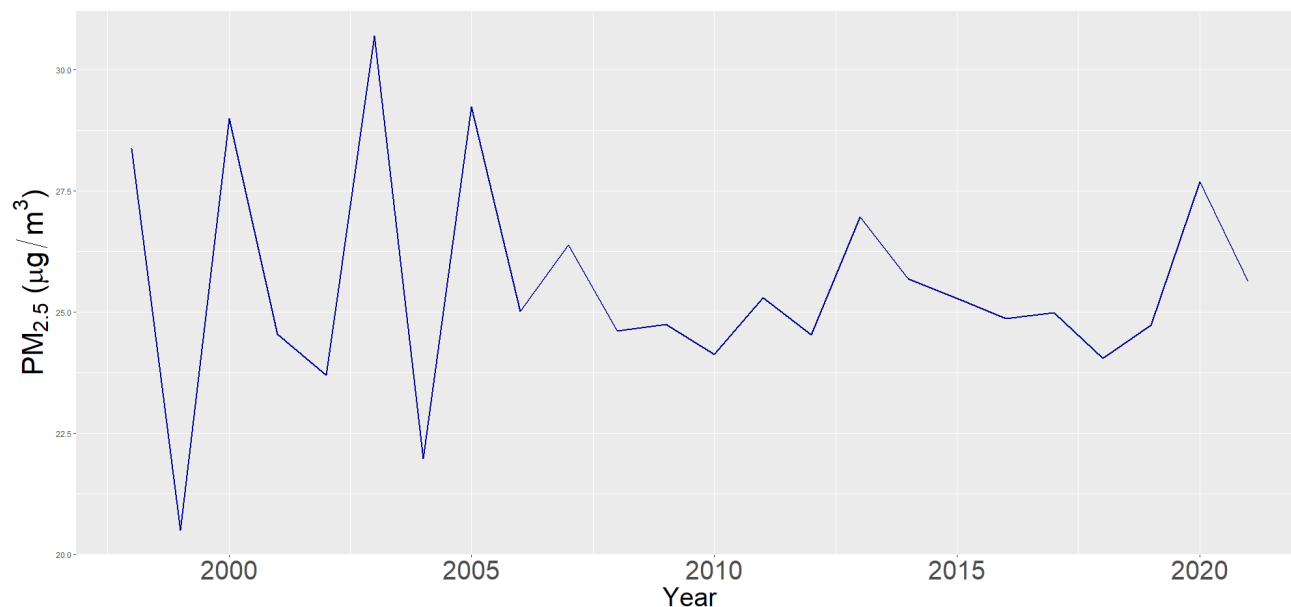


**Fig 7.** Trends in yearly-averaged PM<sub>2.5</sub> in Guatemala between 1998-2021.

Along with calculating the annual and monthly averages for all of Guatemala, we also dove deeper into the dataset and calculated the annual and monthly averages for each department within Guatemala. This 24-year-long analysis revealed that the department Sacatepéquez has the highest PM<sub>2.5</sub> concentrations compared to all the other departments across the entire time period between 1998-2021 (Figure 8 & Table 2). Sacatepéquez is a major tourist destination and is located directly adjacent to the capital city of the country. This department has an annual average PM<sub>2.5</sub> concentration of 40 µg/m<sup>3</sup>, which is twice as high as the lowest annual average concentration estimated in Petén and 6 µg/m<sup>3</sup> higher than the second-highest annual concentration estimated in the department of Guatemala.

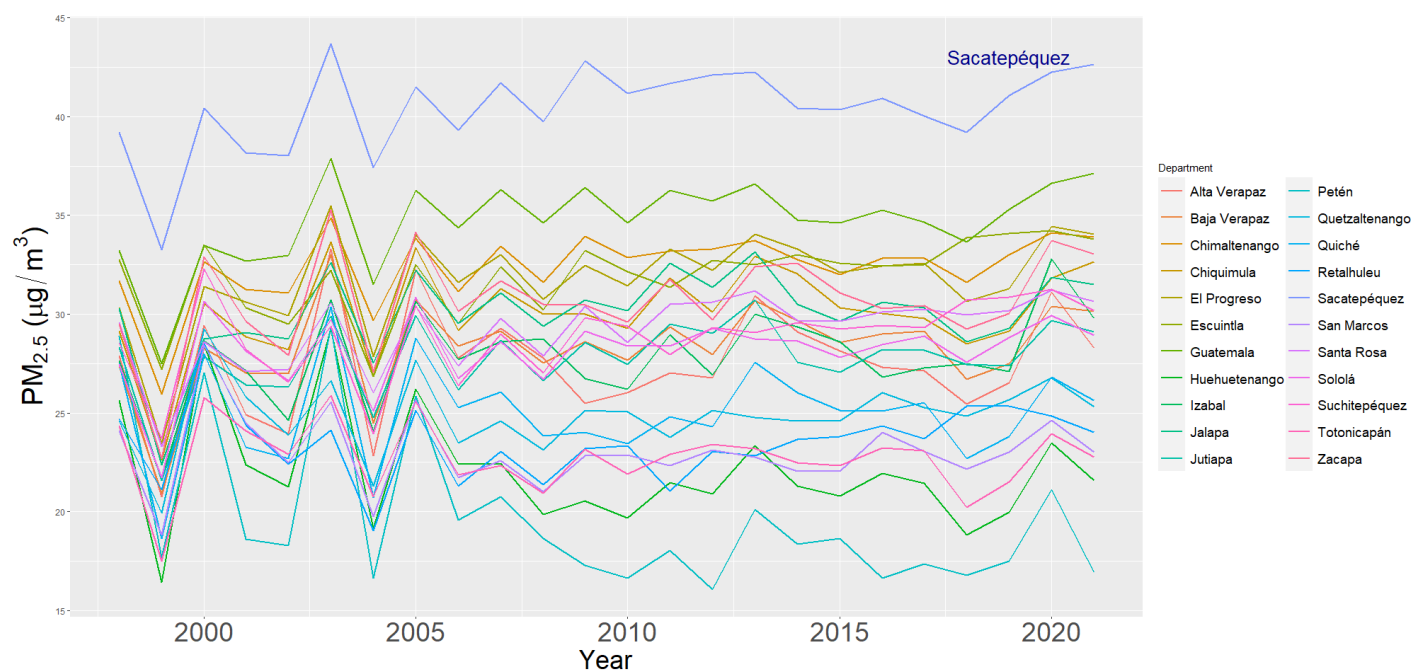
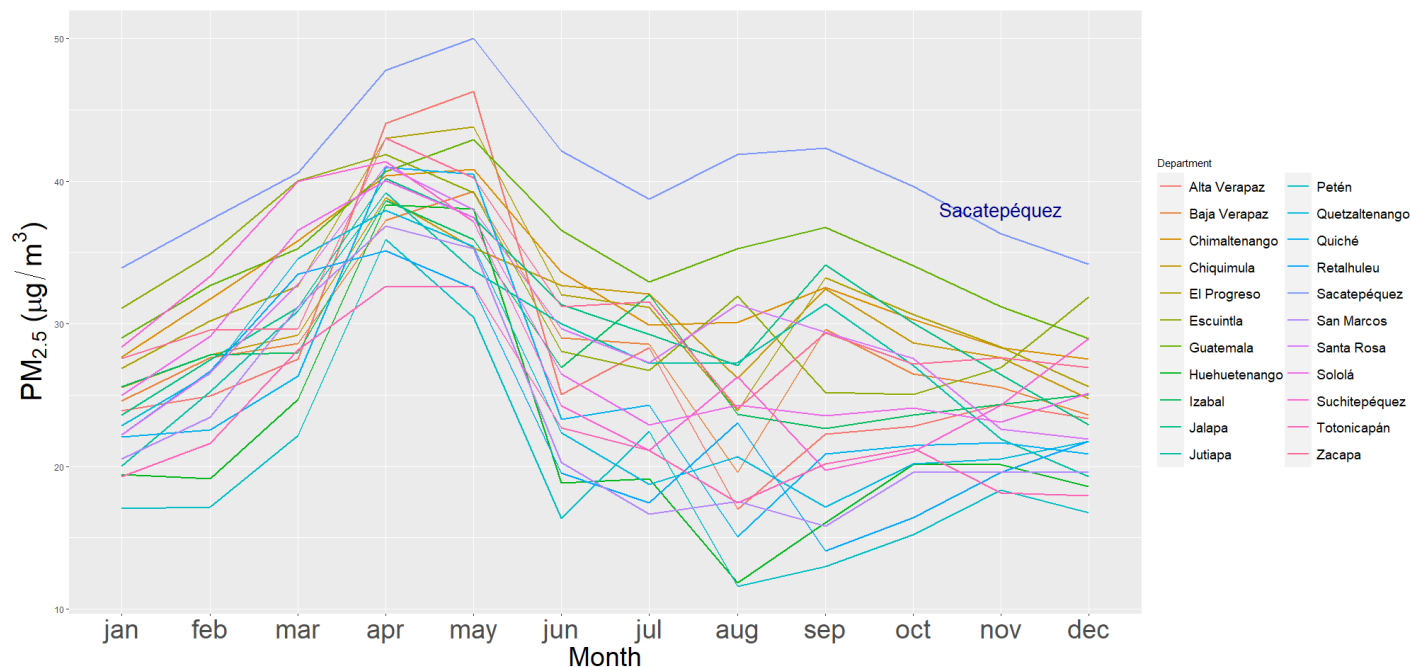


**Fig 8.** Trends in yearly-averaged  $PM_{2.5}$  by department in Guatemala between 1998-2021. The department Sacatepéquez with the highest concentrations is represented by the top line in blue and is indicated by its label above. The line representing Guatemala is for the Department of Guatemala, not the entire country.

**Table 2.** Summary statistics of the annual average PM<sub>2.5</sub> concentrations between 1998-2021 for each department within Guatemala. The average, standard deviation (SD), minimum (Min), first quartile (Q1), median (Med), third quartile (Q3), and maximum (Max) are listed.

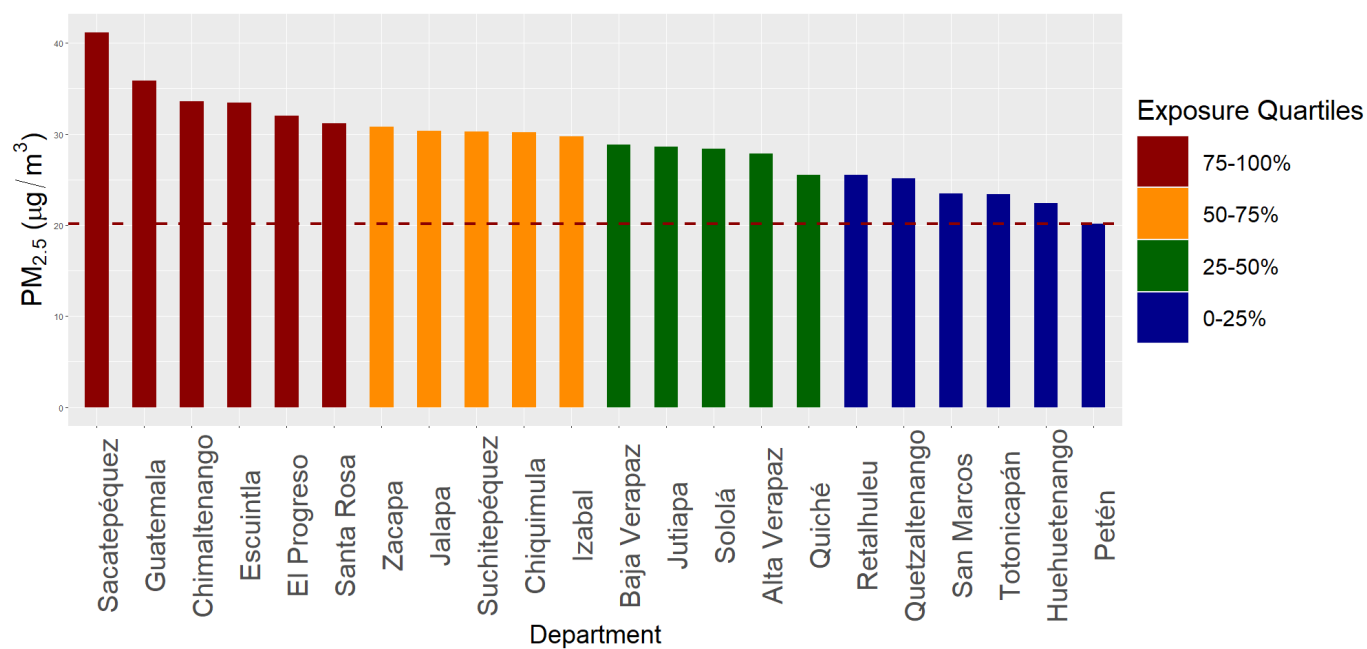
<b>Department</b>	<b>Average</b>	<b>SD</b>	<b>Min</b>	<b>Q1</b>	<b>Med</b>	<b>Q3</b>	<b>Max</b>
<b>Sacatepéquez</b>	40.39	2.21	33.26	39.28	40.67	41.81	43.66
<b>Guatemala</b>	34.68	2.18	27.48	33.6	34.72	36.28	37.88
<b>Chimaltenango</b>	32.39	1.83	25.96	31.62	32.83	33.52	34.89
<b>Escuintla</b>	31.89	1.99	26.85	31.09	32.5	33.06	34.23
<b>El Progreso</b>	31.78	2.45	23.46	30.73	32.18	33.29	35.48
<b>Zacapa</b>	30.66	2.58	22.71	29.64	30.45	32.46	35.26
<b>Chiquimula</b>	30.09	2.34	22.63	29.15	30.03	31.83	33.66
<b>Jalapa</b>	30.08	2.19	22.36	29.23	30.3	31.4	33.15
<b>Santa Rosa</b>	29.2	1.88	23.31	28.4	29.87	30.41	31.2
<b>Suchitepéquez</b>	28.82	2.08	23.69	28.15	29.33	29.91	32.29
<b>Baja Verapaz</b>	28.3	2.32	20.92	27.46	28.47	29.44	33.02
<b>Sololá</b>	28.14	1.89	21.74	27.54	28.52	28.99	30.87
<b>Izabal</b>	27.84	2.33	21.66	26.9	27.67	29.05	32.78
<b>Jutiapa</b>	27.77	1.93	21.58	26.94	28	29.07	30.73
<b>Alta Verapaz</b>	27.48	2.88	20.77	25.89	27.55	29.15	33.31
<b>Quiché</b>	25	2.55	18.64	23.71	25.11	26.26	30.35
<b>Quetzaltenango</b>	24.88	1.88	19.95	24.41	24.95	25.7	29.25
<b>Retalhuleu</b>	23.49	1.91	19.03	22.74	23.68	24.46	28.54
<b>San Marcos</b>	23.02	1.95	18.84	22.12	22.85	24.05	28.44
<b>Totonicapán</b>	22.76	1.84	17.52	21.9	22.92	23.54	25.87
<b>Huehuetenango</b>	22.03	2.95	16.42	20.4	21.46	22.68	29.24
<b>Petén</b>	19.7	3.96	16.07	17.2	18.34	20.27	29.35

Figure 9 shows the monthly trends in PM<sub>2.5</sub> concentrations for each department between 1998-2021. Following the overall trend for the entire country (Figure 6), all departments have spikes during the spring months, specifically April and May. The concentrations ranged between about 12  $\mu\text{g}/\text{m}^3$  and 50  $\mu\text{g}/\text{m}^3$ , with Petén being the department that reaches the minimum concentration and the Sacatepéquez being the department that reaches the maximum concentration.



**Fig 9.** Trends in monthly-averaged  $PM_{2.5}$  by department in Guatemala between 1998-2021. The department Sacatepéquez with the highest concentrations is indicated by its label above. The line representing Guatemala is for the Department of Guatemala, not the entire country.

Figure 10 & Table 3 show the average population-weighted exposure to  $PM_{2.5}$  by department. To classify each department based on lowest to highest exposure, the different colors in the bar plot represent different exposure quartiles between the highest and lowest population-weighted exposure to  $PM_{2.5}$ . The departments with the bottom 25% exposure to  $PM_{2.5}$  relative to the other departments were classified in the 0-25% exposure quartile. On the other hand, the departments that ranked in the top 25% of exposure to  $PM_{2.5}$  were classified in the 75-100% exposure quartile. As expected, the department with the highest population-weighted annual average  $PM_{2.5}$  concentrations is Sacatepéquez ( $41 \mu\text{g}/\text{m}^3$ ). The department with the lowest average exposure is Petén ( $20 \mu\text{g}/\text{m}^3$ ). In the entire country of Guatemala, the average exposure to  $PM_{2.5}$  is approximately  $29 \mu\text{g}/\text{m}^3$ .



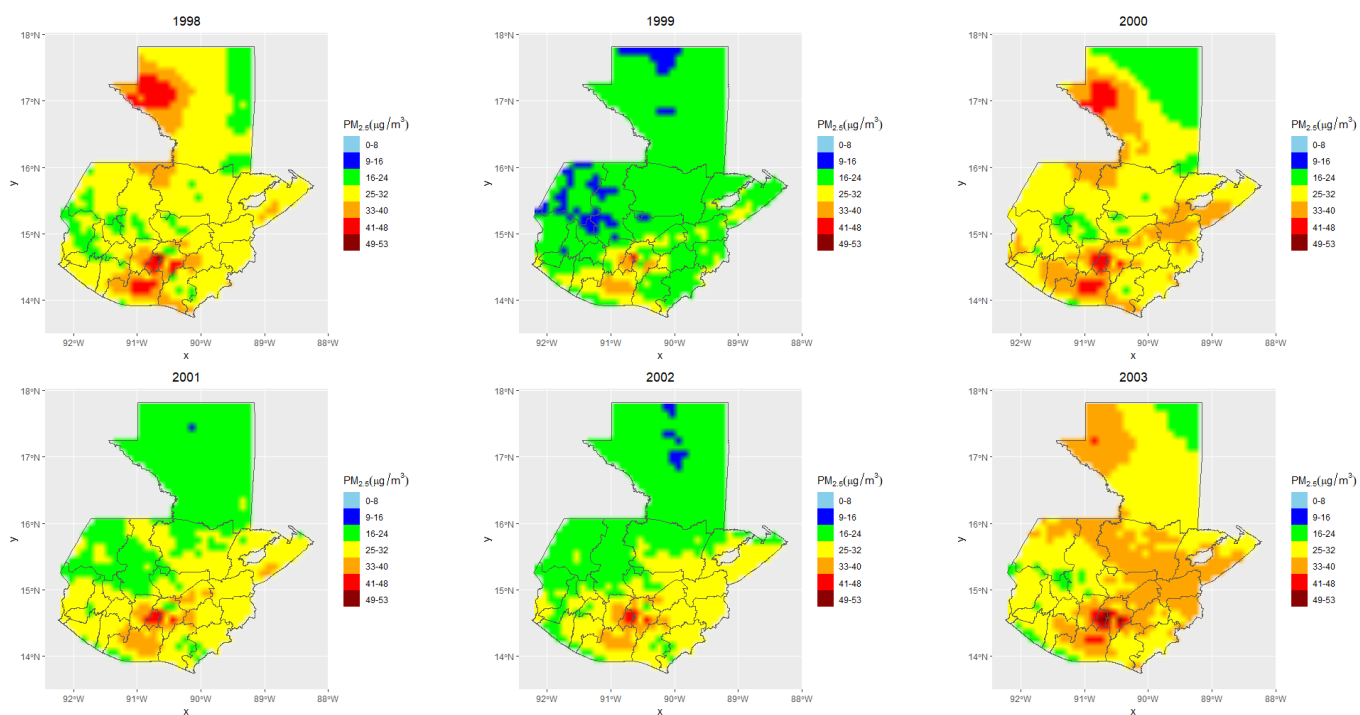
**Fig 10.** Bar plot of the average population-weighted exposure to PM<sub>2.5</sub> by department in Guatemala between 1998-2021. The bar representing Guatemala is for the Department of Guatemala, not the country itself. The dashed line across the plot is a reference line for the difference in the magnitude of exposure that each department experiences relative to the least exposed department, Petén.

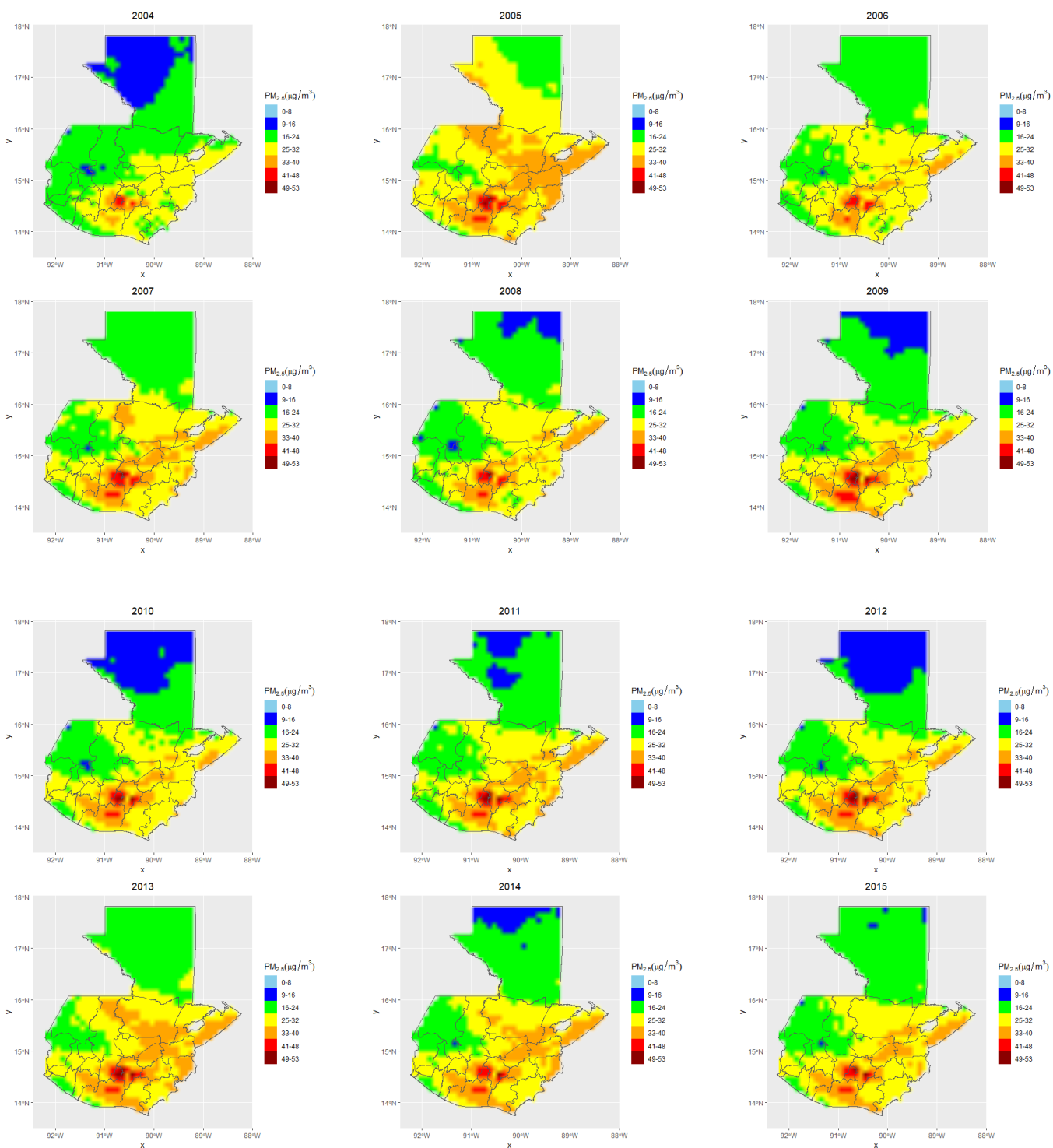
**Table 3.** Summary statistics of the population-weighted yearly average exposure to PM<sub>2.5</sub> concentrations between 1998-2021 for each department within Guatemala. The average, standard deviation (SD), minimum (Min), first quartile (Q1), median (Med), third quartile (Q3), and maximum (Max) are all listed.

<b>Department</b>	<b>Average</b>	<b>SD</b>	<b>Min</b>	<b>Q1</b>	<b>Med</b>	<b>Q3</b>	<b>Max</b>
<b>Sacatepéquez</b>	41.16	2.20	34.15	40.23	41.44	42.64	44.35
<b>Guatemala</b>	35.83	2.13	28.87	34.79	35.86	37.34	38.90
<b>Chimaltenango</b>	33.57	1.85	27.17	32.85	33.96	34.77	35.95
<b>Escuintla</b>	33.43	2.04	28.41	32.77	34.02	34.50	35.95
<b>El Progreso</b>	31.99	2.45	23.71	30.94	32.35	33.49	35.68
<b>Santa Rosa</b>	31.20	1.97	25.18	30.28	31.95	32.46	33.30
<b>Zacapa</b>	30.78	2.61	22.77	29.73	30.59	32.57	35.36
<b>Jalapa</b>	30.37	2.19	22.63	29.56	30.56	31.74	33.44
<b>Suchitépéquez</b>	30.28	2.16	25.04	29.51	30.79	31.59	33.73
<b>Chiquimula</b>	30.20	2.35	22.75	29.25	30.13	31.95	33.78
<b>Izabal</b>	29.77	2.53	22.86	28.80	29.48	31.28	34.95
<b>Baja Verapaz</b>	28.86	2.34	21.51	27.99	28.99	29.97	33.42
<b>Jutiapa</b>	28.62	1.96	22.44	27.79	28.86	29.92	31.63
<b>Sololá</b>	28.39	1.87	22.04	27.89	28.76	29.27	31.05
<b>Alta Verapaz</b>	27.82	2.88	20.92	26.31	27.90	29.55	33.47
<b>Quiché</b>	25.54	2.62	19.19	24.28	25.57	27.04	30.86
<b>Retalhuleu</b>	25.49	2.00	20.72	24.74	25.70	26.44	30.71
<b>Quetzaltenango</b>	25.09	1.88	20.23	24.55	25.33	25.95	29.41
<b>San Marcos</b>	23.47	1.92	19.23	22.67	23.45	24.34	28.67
<b>Totonicapán</b>	23.38	1.78	18.33	22.54	23.48	24.35	26.34
<b>Huehuetenango</b>	22.41	2.98	16.70	20.70	21.81	23.16	29.69
<b>Petén</b>	20.14	4.22	16.50	17.52	18.62	20.68	30.17

In Figure 11, we can see the spatial distribution of PM<sub>2.5</sub> concentrations across the entire country for each year at a 0.1° x 0.1° resolution. As expected, there are always relatively high concentrations near the capital city of Guatemala, the department of Guatemala, Chimaltenango, and Escuintla. Between 1998-2021 the highest annual PM<sub>2.5</sub> concentrations for each of these departments (along with the year in which they occurred) are as follows: 44 µg/m<sup>3</sup> (1998), 38 µg/m<sup>3</sup> (2003), 43 µg/m<sup>3</sup> (2020), and 34 µg/m<sup>3</sup> (2020), respectively. Outside of these areas, there

were moderately higher concentrations near the eastern departments, including El Progreso, Zacapa, Izabal, and near the southern border of Alta Verapaz. The highest annual  $PM_{2.5}$  concentrations for these departments were:  $35 \mu\text{g}/\text{m}^3$  (2003),  $35 \mu\text{g}/\text{m}^3$  (2003),  $33 \mu\text{g}/\text{m}^3$  (2020),  $33 \mu\text{g}/\text{m}^3$  (2003).





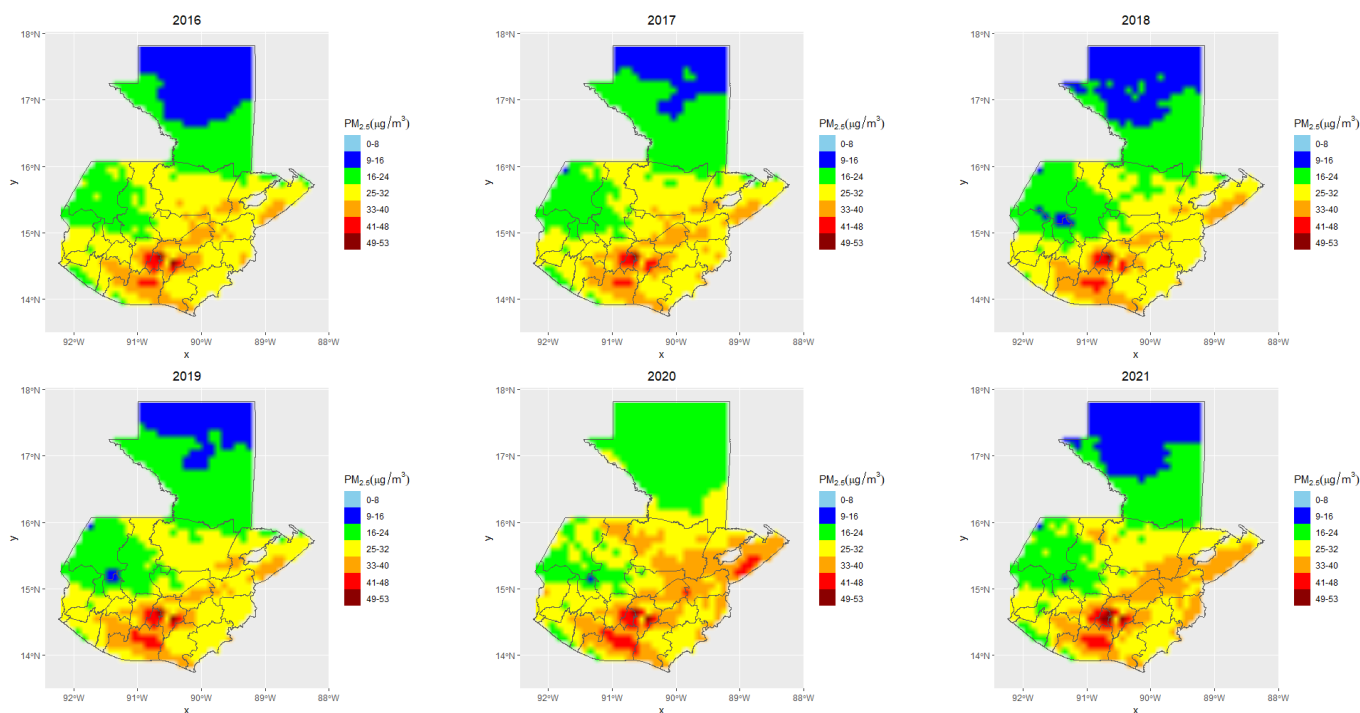
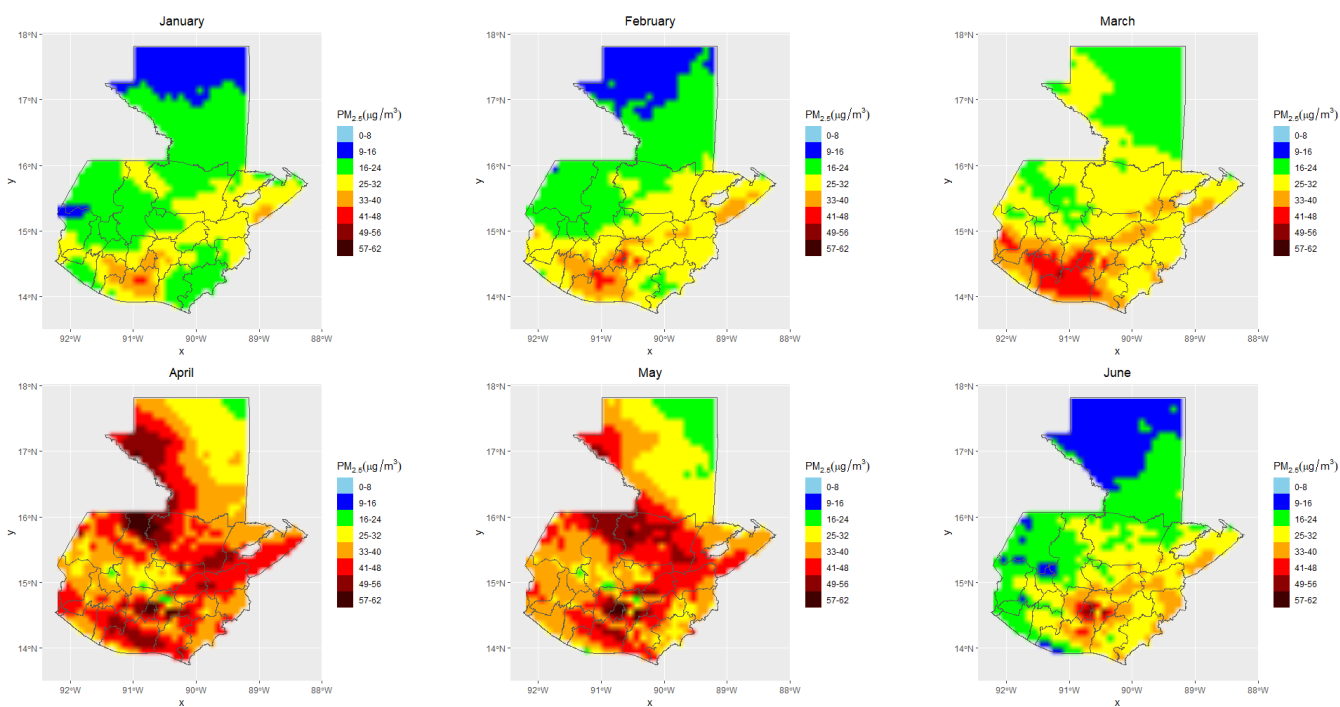


**Fig 11.** Spatial maps of yearly average  $PM_{2.5}$  concentrations in Guatemala between 1998- 2021.

More specifically, Figure 12 illustrates the spatial distribution of  $PM_{2.5}$  concentrations on a monthly basis. Just like the yearly plots (Figure 11), we are seeing high concentrations year-round in the regions near the capital city; however, these monthly plots show very different spatial patterns in the spring months compared to the annual averages. As found previously (Figures 6 and 9), there are spikes in  $PM_{2.5}$  concentrations occurring around March-May, and these monthly figures indicate that these spikes are occurring both near the capital city as well as in the northern departments such as Alta Verapaz, Quiché, and Petén (on the west side). The maximum monthly  $PM_{2.5}$  concentrations for each of these three departments (along with the month in which they occur) are as follows:  $46 \mu\text{g}/\text{m}^3$  (May),  $41 \mu\text{g}/\text{m}^3$  (April), and  $36 \mu\text{g}/\text{m}^3$  (April), respectively. It is interesting to note that these regions tend to have lower  $PM_{2.5}$  concentrations throughout the rest of the year. In fact, some of the lowest monthly concentrations occur in these same departments. Petén, for instance, has the absolute lowest monthly average

out of all the departments at  $12 \mu\text{g}/\text{m}^3$  (August), Quiché has the 5<sup>th</sup> lowest monthly average at  $15 \mu\text{g}/\text{m}^3$  (August), and Alta Verapaz has the 13<sup>th</sup> lowest monthly average at  $16 \mu\text{g}/\text{m}^3$  (August).

This suggests that there is an emissions source that is impacting these regions during the spring but not during the other seasons.



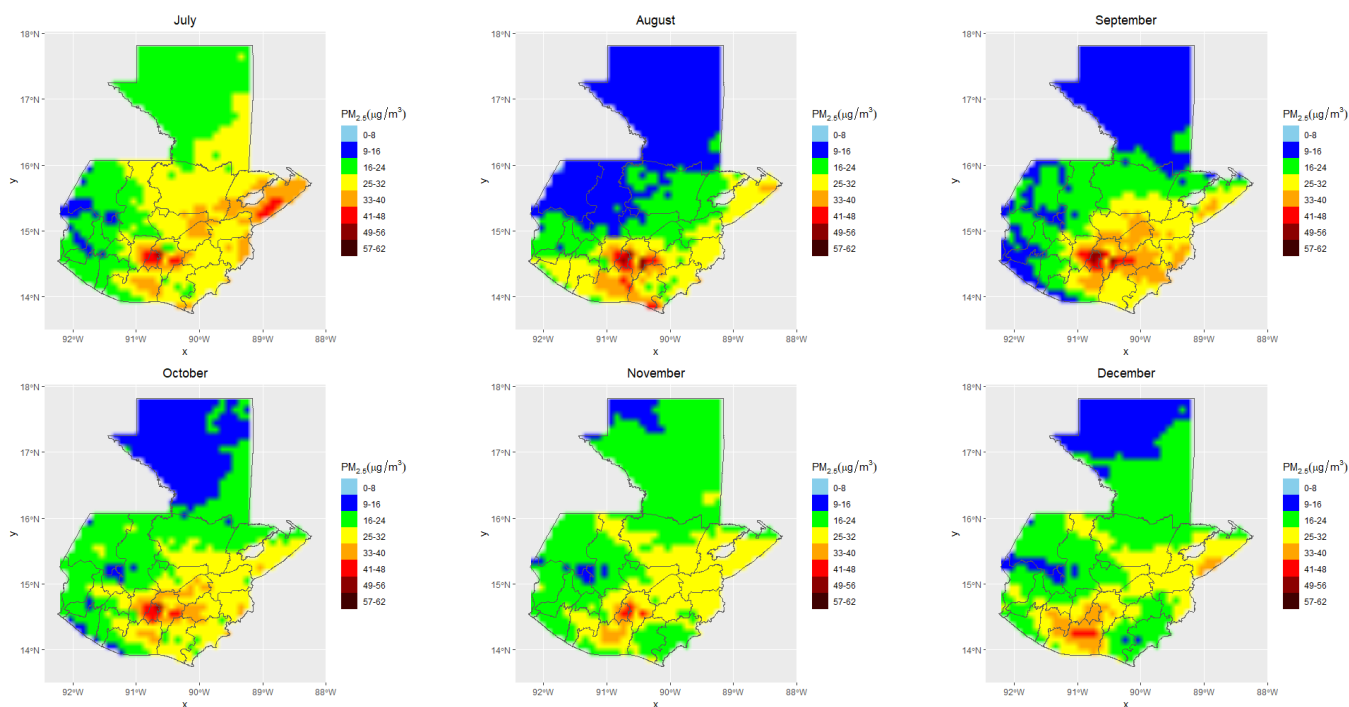


**Fig 12.** Spatial maps of monthly average  $PM_{2.5}$  concentrations in Guatemala between 1998- 2021.

The analysis of each emissions source reveals that there is a large variability in the relative contributions of each source to  $PM_{2.5}$  mass concentrations (Table 4 & Figure 13). Aside from other sources than the ones specified, residential and commercial sources are the largest contributors to  $PM_{2.5}$  with an average relative contribution of 23% (Table 4). Biomass burning is the second largest contributor with an average contribution of 18%. As shown in Figure 13, commercial and residential sources are increasing  $PM_{2.5}$  in the mid-west of the country, including the regions near the capital city. Biomass burning makes its biggest impact in Petén, compared to the other departments, especially near the western border. It is interesting to note that this is exactly where we see high  $PM_{2.5}$  values in the spatial maps (Figure 12) during the spring months when  $PM_{2.5}$  concentrations peak. These top three sources (other, residential/commercial, and biomass burning) are major contributors compared to the rest of the sources because they account for a total of 66% of the  $PM_{2.5}$  in the country. On the other hand,

the bottom three sources include dust, agricultural activity (excluding biomass burning), and wind erosion with relative contributions amounting to 2%, 3%, and 3%, respectively. Wind erosion and agricultural activity seem to affect the lower portion of the country near the southern border, while dust affects a couple of regions on the western border.

**Table 4.** Summary statistics of the relative contributions of each emissions source. The average, standard deviation (SD), minimum (Min), first quartile (Q1), median (Med), third quartile (Q3), and maximum (Max) are listed as percentages. The source profiles include all commercial and residential cooking, lighting, and heating (RESI); biomass burning including agricultural waste burning (BIOB); all transport excluding aviation (TRANS); Energy generation (POWER); waste burning (WASTE); all industries and product use (INDUS); wind erosion (WINDUST); agricultural activities excluding agricultural waste burning (AGR); anthropogenic dust (DUST); and all other sources (OTHER).

<b>Source</b>	<b>Average</b>	<b>SD</b>	<b>Min</b>	<b>Q1</b>	<b>Med</b>	<b>Q3</b>	<b>Max</b>
<b>OTHER</b>	25.34	11.42	8.53	15.67	22.71	31.87	50.67
<b>RESI</b>	22.89	15.46	4.54	8.39	20.64	34.79	63.44
<b>BIOB</b>	17.87	14.37	3.04	5.81	11.00	28.20	56.83
<b>TRANS</b>	8.92	2.73	4.87	7.17	7.80	10.28	15.45
<b>POWER</b>	8.64	4.45	2.41	5.60	6.93	11.79	24.59
<b>WASTE</b>	4.46	1.99	1.30	2.62	4.61	6.08	8.55
<b>INDUS</b>	3.56	1.76	1.30	2.01	3.28	4.49	10.23
<b>WINDUST</b>	3.15	3.79	0.24	0.84	1.30	3.09	14.91
<b>AGR</b>	2.74	1.60	0.71	1.51	2.13	3.65	7.21
<b>DUST</b>	2.43	0.78	1.11	2.07	2.23	2.61	5.08

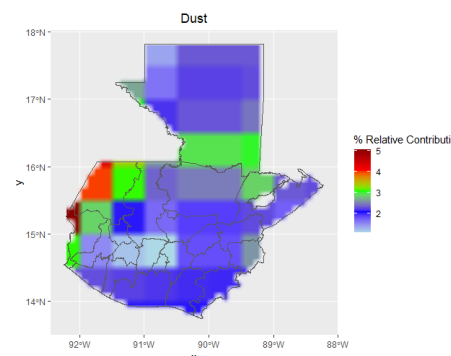
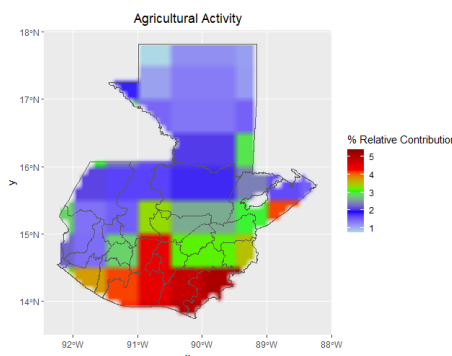
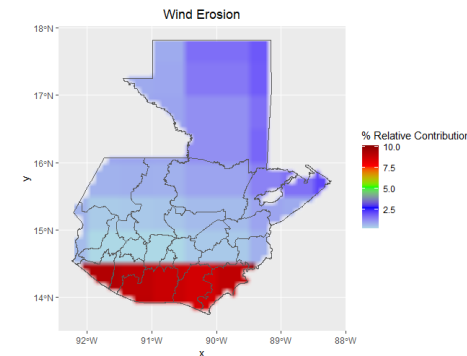
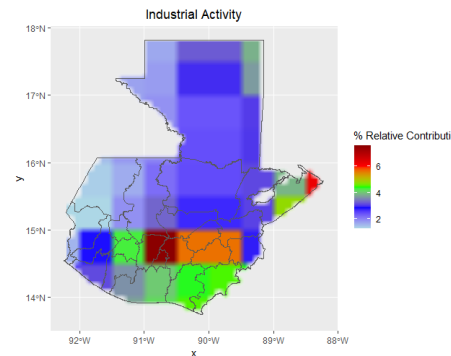
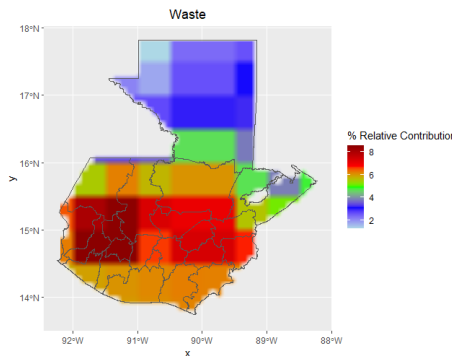
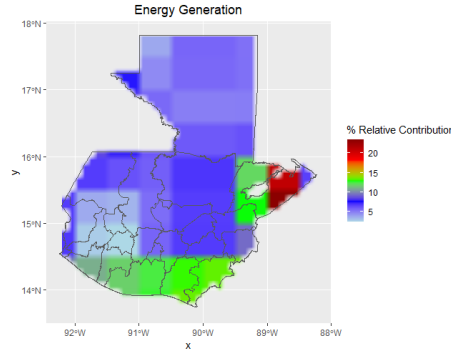
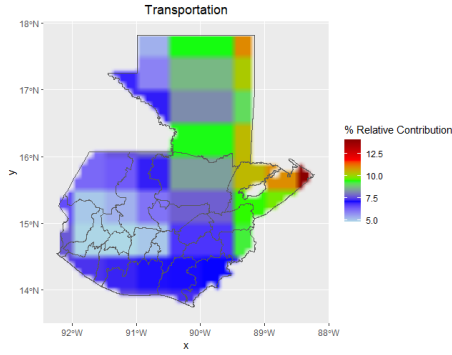
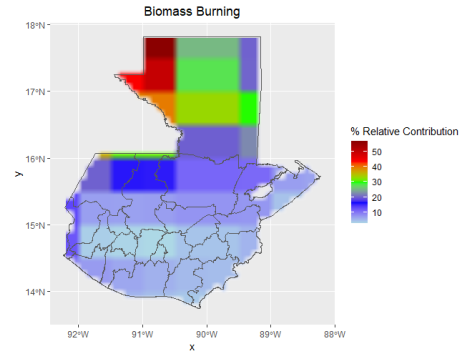
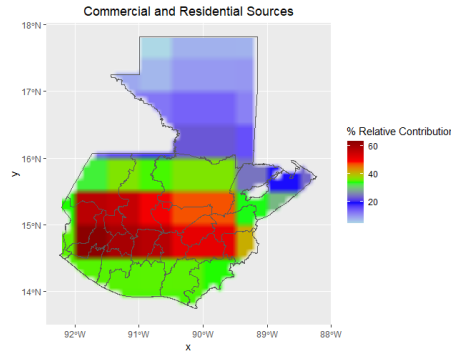
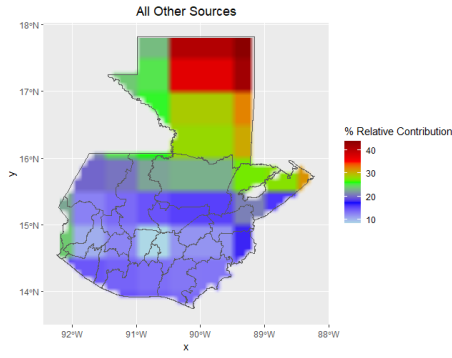


**Fig 13.** Spatial maps of the relative contributions from each emissions source. The above figures represent all other, commercial and residential, biomass burning (including agricultural waste), transportation, energy generation, waste, industrial activity, wind erosion, agricultural activity (excluding agricultural waste burning), and dust sources.

### E-Sampler vs Satellite

The comparison between the e-sampler measurements and the satellite-derived measurements shows that there are major differences between the two data sets. The paired t-test between the e-sampler with a 100% data threshold and the satellite data at  $0.1^\circ \times 0.1^\circ$  and  $0.01^\circ \times 0.01^\circ$  resolutions results in statistically significant differences ( $p\text{-value} < 2.2 \times 10^{-16}$ ,  $p\text{-value} = 2.211 \times 10^{-11}$ , respectively). The satellite-derived data has higher mean concentrations than the e-sampler measurements, with differences at the two resolutions being  $23.7 \mu\text{g}/\text{m}^3$  and  $20.4 \mu\text{g}/\text{m}^3$  higher, respectively. However, Figure 14 shows that the overall trends in  $\text{PM}_{2.5}$  variations are quite similar for the satellite-derived data compared to the e-sampler data. In this time series plot, it is noticeable that there are two spikes that occur throughout the 2018- 2021 period, and both spikes are occurring during the Spring months for both data sources.

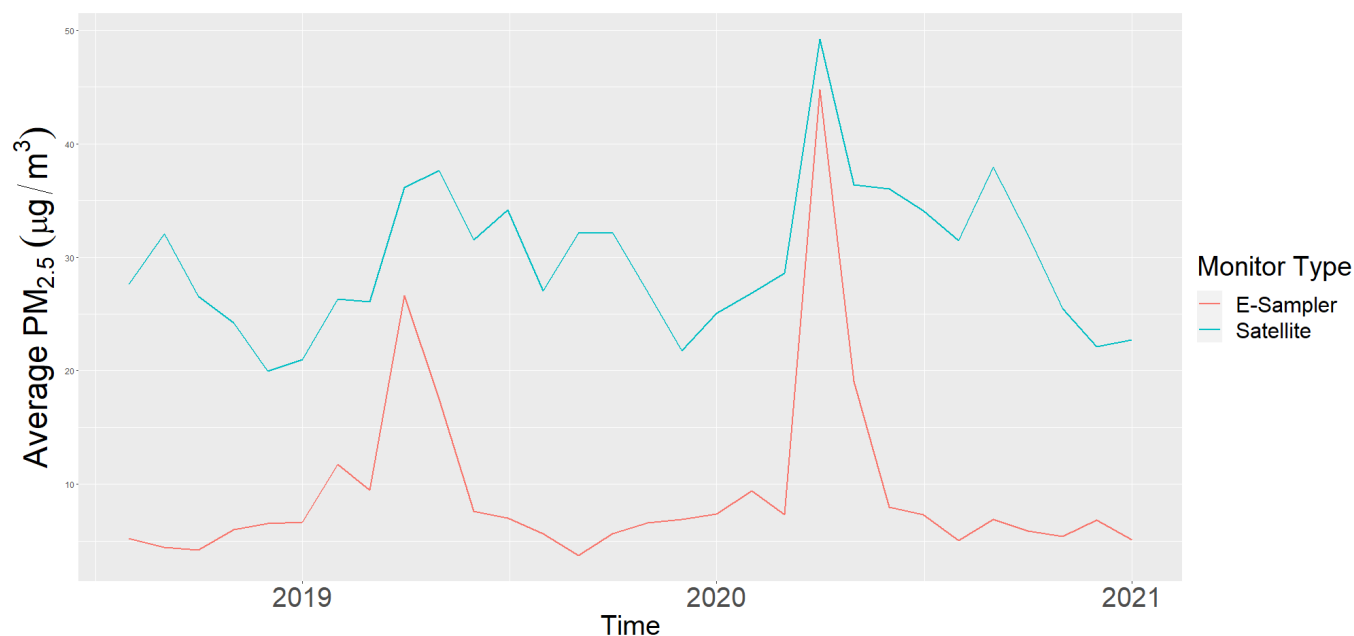


**Fig 14.** Comparison of the e-sampler and satellite-derived monthly-averaged  $PM_{2.5}$  in Guatemala between 2018-2021. The e-sampler measurements are in red and the  $0.01^\circ \times 0.01^\circ$  resolution satellite-derived measurements at latitude 14.65 and longitude -90.15 are in blue.

## Discussion

The future direction for communities in Guatemala may be related to composting crop residues that would otherwise be burned. The satellite-based estimates showed that when there are high  $PM_{2.5}$  concentrations, they tend to lie on the western side of Petén and the northwestern side of the whole country. Near these same areas is exactly where the analysis of the relative contributions of each emissions source showed that there are high levels of biomass burning. Biomass burning includes the burning of crop residue, which is an agricultural byproduct of harvesting crops (Obi et al., 2016). In the departments where high  $PM_{2.5}$  concentrations were detected by the satellite-derived estimates, crops such as African palm are produced (FEWSN, 2016). In Guatemala, this crop is harvested from January to April, which is approximately when the spikes in  $PM_{2.5}$  concentrations occurred, as evidenced by both the e-sampler measurements

and satellite-derived data (*Viceministerio de Sanidad Agropecuaria y Regulaciones*, n.d.). Based on the spatial and temporal linkage, it is possible that the burning of crop residue such as African palm is contributing to high PM events in Guatemala.

Unfortunately, crop residue can have a serious negative impact on air pollution when managed via burning (Bellarby et al., 2008). A major reason why crop residue is not managed properly can be understood by comparing the agricultural waste system to that of municipal solid waste (MSW). MSW is sometimes handled by the public sector, with governing organizations keeping track of the amount of waste generated and disposing of it properly. However, agricultural waste is typically managed by each farmer rather than through a centralized body. This puts the responsibility of the waste on private entities. Although harvest waste can be upcycled to produce other products such as paper, the cost of transporting and processing this waste can be more expensive than simply burning it in the field (Bhuvaneshwari et al., 2019). It is theoretically possible for crop waste to be managed by public instead of private entities, such as those that collect and dispose of municipal solid waste. This type of system would remove pressure from farmers and ensure that harvest waste is dealt with in a way that is suitable for the community. However, not all regions in developing countries have access to MSW collection services. In Guatemala, about 32% of the population is not covered by waste collection services (What a Waste Global Database | Data Catalog, 2023). So, if a service that is typical for a government to provide is not available, then the likelihood that an agricultural waste collection service will be successfully implemented by the government is low.

However, managing crop residue in a sustainable way can be very difficult for farmers to do on their own without government assistance. If farmers wanted to, for example, sell their harvest waste for use at a paper-producing facility, transporting the waste to the next facility will

have a high upfront cost that can be avoided by simply burning the crops. Therefore, managing the waste onsite at the farm is the easiest and cheapest alternative to crop burning (Bhuvaneshwari et al., 2019). One possible on-site option for farmers dealing with crop waste is composting. Composting is the process of decomposing organic matter into a soil amendment that improves soil fertility. By utilizing compost as a soil amendment, farmers typically see improved crop yields and resistance to external factors such as pests and drought (Misra et al., 2003). To address the need for composting infrastructure in Guatemala, a study by Achilias (2022) found that using the “in-cell technique” instead of windrows in Guatemala for composting was cheaper, without requiring expensive equipment such as a tractor and windrow turner for turning and churning. This could be a fair option for other farmers in Guatemala who do not have the resources to purchase advanced equipment for composting.

In addition to reducing emissions, adding compost to soil greatly improves soil fertility by reinforcing microbial communities and adding to the nutrient content, which results in enhanced crop biomass and growth (Calleja-Cervantes et al., 2015). A study by Wittman & Johnson (2008) that interviewed farmers in Guatemala found that most farmers have noticed a drop in soil fertility over the course of their lifetimes. Two-thirds of those interviewed in San Pedrito and San Antonio, Guatemala have seen lowered crop yields despite the use of synthetic fertilizers. Therefore, the benefits of switching from burning crops to composting them could be a great way to not only reduce  $PM_{2.5}$  emissions but also to fertilize the soil and improve crop yields for farmers. Composting is cost-effective and can be done onsite at a farm by using the same crop residues that farmers need to dispose of, so this may be the best next step for farmers in Guatemala who will otherwise burn their crop residues.

## Conclusion

Based on both the on-the-ground e-sampler and the satellite-derived data, there has clearly been a spike in PM<sub>2.5</sub> concentrations occurring during the spring months in Guatemala for at least the past two decades. The annual average concentrations between 1998-2021 vary between 16-44  $\mu\text{g}/\text{m}^3$  depending on the department, and these values are 3-9x higher than the WHO's recommended annual mean concentrations of 5  $\mu\text{g}/\text{m}^3$  (*WHO Global Air Quality Guidelines*, 2021). At its worst, the highest raw 5-minute PM<sub>2.5</sub> observation recorded by the e-sampler reached 835  $\mu\text{g}/\text{m}^3$ .

The PM<sub>2.5</sub> monitoring in this country is weak and needs to be enhanced, especially in the context of satellite-based modeling techniques that can predict PM<sub>2.5</sub> measurements given enough ground-based monitors. The limitation of this study is related to the lack of a sufficient number of ground-based measurements available. Based on a mean difference of about 20  $\mu\text{g}/\text{m}^3$  between the satellite and e-sampler measurements, there are not enough on-the-ground air quality monitors in this country to satisfy the requirements of an accurate model. Although the PM<sub>2.5</sub> estimates developed by van Donkelaar et al. (2021) merged ground-based monitors, satellite estimates, and chemical model simulations to determine the best PM<sub>2.5</sub> estimates with less uncertainty than each technique alone, the lack of monitors in Central America still led to higher levels of uncertainty than monitor-dense regions, such as North America (Diao et al., 2019; van Donkelaar et al., 2021). Furthermore, surface PM<sub>2.5</sub> in regions heavily affected by biomass burning events is also more difficult to estimate using AOD retrievals than when there are clearer skies (van Donkelaar et al., 2021). Since biomass burning is heavy in parts of Guatemala, this further supports the need for additional ground-based monitors in this country. Along with reinforcing satellite-based estimates of surface PM<sub>2.5</sub>, ground-based monitors in

general can have a great impact on communities in the form of advising epidemiological studies, air pollution regulatory decisions, emissions inventories, and responses to extreme events such as wildfires (Diao et al., 2019). Therefore, the next steps for research in this country should focus on improving monitor density, especially in areas heavily affected by biomass burning, to make sure there is enough data to make informed decisions. Despite a significant difference between the two data sources, the seasonal trends remain similar. So, the satellite data may be useful for detecting patterns, but the absolute measurements must be bias-corrected to determine true exposure levels.

## References:

1. Achilias, D. S. (2022). *Waste Material Recycling in the Circular Economy: Challenges and Developments*. BoD – Books on Demand.
2. Bellarby, J., Foereid, B., Hastings, A. F. S. J., & Smith, P. (2008). *Cool Farming: Climate impacts of agriculture and mitigation potential*.  
<https://abdn.pure.elsevier.com/en/publications/cool-farming-climate-impacts-of-agriculture-and-mitigation-potent>
3. Bhuvaneshwari, S., Hettiarachchi, H., & Meegoda, J. N. (2019). Crop Residue Burning in India: Policy Challenges and Potential Solutions. *International Journal of Environmental Research and Public Health*, 16(5), 832. <https://doi.org/10.3390/ijerph16050832>
4. Calleja-Cervantes, M. E., Fernández-González, A. J., Irigoyen, I., Fernández-López, M., Aparicio-Tejo, P. M., & Menéndez, S. (2015). Thirteen years of continued application of composted organic wastes in a vineyard modify soil quality characteristics. *Soil Biology and Biochemistry*, 90, 241–254. <https://doi.org/10.1016/j.soilbio.2015.07.002>
5. Carslaw, D. C., & Ropkins, K. (2012). openair — An R package for air quality data analysis. *Environmental Modelling & Software*, 27–28, 52–61.  
<https://doi.org/10.1016/j.envsoft.2011.09.008>
6. Diao, M., Holloway, T., Choi, S., O'Neill, S. M., Al-Hamdan, M. Z., van Donkelaar, A., Martin, R. V., Jin, X., Fiore, A. M., Henze, D. K., Lacey, F., Kinney, P. L., Freedman, F., Larkin, N. K., Zou, Y., Kelly, J. T., & Vaidyanathan, A. (2019). Methods, availability, and applications of PM<sub>2.5</sub> exposure estimates derived from ground measurements, satellite, and atmospheric models. *Journal of the Air & Waste Management Association* (1995), 69(12), 1391–1414. <https://doi.org/10.1080/10962247.2019.1668498>

7. FAO, I. (2014). Strengthening the enabling environment for food security and nutrition. *The State of Food Insecurity in the World*, 1-57.
8. FEWSNET (2016). Guatemala Livelihood zone profiles. *FEWS NET*. (2016).  
<https://fewsn.net/central-america-and-caribbean/guatemala/livelihood-description/november-2016>
9. Fuller, R., Landrigan, P. J., Balakrishnan, K., Bathan, G., Bose-O'Reilly, S., Brauer, M., Caravanos, J., Chiles, T., Cohen, A., Corra, L., Cropper, M., Ferraro, G., Hanna, J., Hanrahan, D., Hu, H., Hunter, D., Janata, G., Kupka, R., Lanphear, B., ... Yan, C. (2022). Pollution and health: a progress update. *The Lancet Planetary Health*, 6(6), e535–e547. [https://doi.org/10.1016/S2542-5196\(22\)00090-0](https://doi.org/10.1016/S2542-5196(22)00090-0)
10. GBD Risk Factor Collaborators (2020). Global burden of 87 risk factors in 204 countries and territories, 1990–2019: a systematic analysis for the Global Burden of Disease Study 2019. *The Lancet*, 396(10258), 1223-1249.
11. *Guatemala Fires 2020 / NASA Applied Sciences*. (2020, April 1).  
<http://appliedsciences.nasa.gov/what-we-do/disasters/disasters-activations/guatemala-fires-2020>
12. Guttikunda, S., & Ka, N. (2022). Evolution of India's PM2.5 pollution between 1998 and 2020 using global reanalysis fields coupled with satellite observations and fuel consumption patterns. *Environmental Science: Atmospheres*, 2(6), 1502–1515.  
<https://doi.org/10.1039/D2EA00027J>
13. Lopez-Ridaura, S., Barba-Escoto, L., Reyna-Ramirez, C., Hellin, J., Gerard, B., & Van Wijk, M. (2019). Food security and agriculture in the Western Highlands of Guatemala. *Food Security*, 11. <https://doi.org/10.1007/s12571-019-00940-z>

14. Manisalidis, I., Stavropoulou, E., Stavropoulos, A., & Bezirtzoglou, E. (2020). Environmental and Health Impacts of Air Pollution: A Review. *Frontiers in Public Health*, 8. <https://www.frontiersin.org/articles/10.3389/fpubh.2020.00014>
15. McDuffie, E. E., Martin, R. V., Spadaro, J. V., Burnett, R., Smith, S. J., O'Rourke, P., Hammer, M. S., van Donkelaar, A., Bindle, L., Shah, V., Jaeglé, L., Luo, G., Yu, F., Adeniran, J. A., Lin, J., & Brauer, M. (2021). Source sector and fuel contributions to ambient PM<sub>2.5</sub> and attributable mortality across multiple spatial scales. *Nature Communications*, 12, 3594. <https://doi.org/10.1038/s41467-021-23853-y>
16. Misra, R. V., Roy, R. N., & Hiraoka, H. (2003). *On-Farm Composting Methods*. <https://vtechworks.lib.vt.edu/handle/10919/65466>
17. Naeher, L. P., Smith, K. R., Leaderer, B. P., Mage, D., & Grajeda, R. (2000). Indoor and outdoor PM<sub>2.5</sub> and CO in high- and low-density Guatemalan villages. *Journal of Exposure Science & Environmental Epidemiology*, 10(6), 544–551. <https://doi.org/10.1038/sj.jea.7500113>
18. Obi, F. O., Ugwuishiwu, B. O., & Nwakaire, J. N. (2016). Agricultural waste concept, generation, utilization and management. *Nigerian Journal of Technology*, 35(4), 957–964. <https://doi.org/10.4314/njt.v35i4>
19. Pérez Orozco, J. J. (2014). *Understanding Farmers' Challenges and Exploring Impacts of a Sustainable Agriculture NGO in Communities of Southern Guatemala* [Master's Field Practicum Report, University of Florida]. University of Florida Digital Collections. <https://original-ufdc.uflib.ufl.edu/AA00061238/00001>
20. Pinder, R. W., Klopp, J. M., Kleiman, G., Hagler, G. S. W., Awe, Y., & Terry, S. (2019). Opportunities and challenges for filling the air quality data gap in low- and middle-

income countries. *Atmospheric Environment*, 215, 116794.

<https://doi.org/10.1016/j.atmosenv.2019.06.032>

21. R Core Team (2022). R: A language and environment for statistical computing. R Foundation for Statistical Computing, Vienna, Austria. URL <https://www.R-project.org/>.
22. Raza, M. H., Abid, M., Faisal, M., Yan, T., Akhtar, S., & Adnan, K. M. M. (2022). Environmental and Health Impacts of Crop Residue Burning: Scope of Sustainable Crop Residue Management Practices. *International Journal of Environmental Research and Public Health*, 19(8), 4753. <https://doi.org/10.3390/ijerph19084753>
23. RStudio Team (2020). RStudio: Integrated Development for R. RStudio, PBC, Boston, MA URL <http://www.rstudio.com/>.
24. Shendell, D. G., & Naeher, L. P. (2002). A pilot study to assess ground-level ambient air concentrations of fine particles and carbon monoxide in urban Guatemala. *Environment International*, 28(5), 375–382. [https://doi.org/10.1016/S0160-4120\(02\)00057-0](https://doi.org/10.1016/S0160-4120(02)00057-0)
25. Valavanidis, A., Fiotakis, K., & Vlachogianni, T. (2008). Airborne Particulate Matter and Human Health: Toxicological Assessment and Importance of Size and Composition of Particles for Oxidative Damage and Carcinogenic Mechanisms. *Journal of Environmental Science and Health, Part C*, 26(4), 339–362.  
<https://doi.org/10.1080/10590500802494538>
26. van Donkelaar, A., Hammer, M. S., Bindle, L., Brauer, M., Brook, J. R., Garay, M. J., Hsu, N. C., Kalashnikova, O. V., Kahn, R. A., Lee, C., Levy, R. C., Lyapustin, A., Sayer, A. M., & Martin, R. V. (2021). Monthly Global Estimates of Fine Particulate Matter and Their Uncertainty. *Environmental Science & Technology*, 55(22), 15287–15300.  
<https://doi.org/10.1021/acs.est.1c05309>

27. *Viceministerio de Sanidad Agropecuaria y Regulaciones*. (n.d.). Retrieved April 11, 2023, from <https://visar.maga.gob.gt/>
28. *What a Waste Global Database | Data Catalog*. (2023). Retrieved February 19, 2023, from <https://datacatalog.worldbank.org/search/dataset/0039597>
29. *WHO global air quality guidelines: Particulate matter (PM<sub>2.5</sub> and PM<sub>10</sub>), ozone, nitrogen dioxide, sulfur dioxide and carbon monoxide*. (2021). World Health Organization. <http://www.ncbi.nlm.nih.gov/books/NBK574594/>
30. Wickham, H. (2016). *ggplot2: Elegant Graphics for Data Analysis*. Springer-Verlag New York.
31. Wittman, H. K., & Johnson, M. S. (2008). Fallow management practices in Guatemala's Western Highlands: social drivers and biophysical impacts. *Land Degradation & Development*, 19(2), 178–189. <https://doi.org/10.1002/ldr.832>
32. World Bank. (2020). *The Global Health Cost of Ambient PM<sub>2.5</sub> Air Pollution*. World Bank. <https://openknowledge.worldbank.org/handle/10986/35721>